



# Rapid carbon accumulation in a peatland following Late Holocene tephra deposition, New Zealand

Joshua L. Ratcliffe<sup>a, b, \*</sup>, David J. Lowe<sup>a</sup>, Louis A. Schipper<sup>a</sup>, Maria J. Gehrels<sup>c, d</sup>,  
Amanda D. French<sup>a</sup>, David I. Campbell<sup>a</sup>

<sup>a</sup> School of Science and Environmental Research Institute, University of Waikato, Private Bag 3105, Hamilton, 3240, New Zealand

<sup>b</sup> Department of Forest Ecology and Management, Swedish University of Agricultural Sciences, Umeå, Sweden

<sup>c</sup> Environment and Geography, University of York, York, YO105DD, UK

<sup>d</sup> School of Geography, The University of Plymouth, Drake Circus, Plymouth, England, PL4 8AA, UK

## ARTICLE INFO

### Article history:

Received 18 March 2020

Received in revised form

20 July 2020

Accepted 20 July 2020

Available online xxx

### Keywords:

Tephrochronology

Volcanism

Nutrients

Geochemistry

Elemental-accumulation

## ABSTRACT

Contemporary measurements of carbon (C) accumulation rates in peatlands around the world often show the C sink to be stronger on average than at times in the past. Alteration of global nutrient cycles could be contributing to elevated carbon accumulation in the present day. Here we examine the effect of volcanic inputs of nutrients on peatland C accumulation in Moanatuatua Bog, New Zealand, by examining a high-resolution Late Holocene C accumulation record during which powerful volcanic eruptions occurred, depositing two visible rhyolitic tephra layers (Taupo,  $232 \pm 10$  CE; Kaharoa,  $1314 \pm 12$  CE). Carbon accumulation rates since c. 50 CE, well before any human presence, increased from a background rate of  $23 \text{ g C m}^{-2} \text{ yr}^{-1}$  up to  $110 \text{ g C m}^{-2} \text{ yr}^{-1}$  following the deposition of the Taupo Tephra, and  $84 \text{ g C m}^{-2} \text{ yr}^{-1}$  following the deposition of the Kaharoa Tephra. Smaller but nevertheless marked increases in C accumulation additionally occurred in association with the deposition of three andesitic-dacitic cryptotephra (each  $\leq 1$  mm thick) of the Tufa Trig Formation between the Taupo and Kaharoa events. These five periods of elevated C uptake, especially those associated with the relatively thick Taupo and Kaharoa tephra, were accompanied by shifts in nutrient stoichiometry, indicating that there was greater availability of phosphorus (P) relative to nitrogen (N) and C during the period of high C uptake. Such P was almost certainly derived from volcanic sources, with P being present in the volcanic glass at Moanatuatua, and many of the eruptions described being associated with the local deposition of the P rich mineral apatite. We found peatland C accumulation to be tightly coupled to N and P accumulation, suggesting nutrient inputs exert a strong control on rates of peat accumulation. Nutrient stoichiometry indicated a strong ability to recover P within the ecosystem, with C:P ratios being higher than most other peatlands in the literature. We conclude that nutrient inputs, deriving from volcanic eruptions, have been very important for C accumulation rates in the past. Therefore, the elevated nutrient inputs occurring in the present day could offer a more plausible explanation, as opposed to a climatic component, for observed high contemporary C accumulation in New Zealand peatlands.

© 2020 Elsevier Ltd. All rights reserved.

## 1. Introduction

The global peatland carbon (C) sink is vast, 644 GT by the most recent estimates (Yu, 2011; Dargie et al., 2017), and greater than all the C content of fossil fuels burnt since 1870 (~435 GT C, as cited in Le Quéré et al., 2018). Peatlands are thus very important for the

global carbon cycle, and there is much interest in the controls of their C uptake and loss. Modern carbon sequestration in peatlands, measured over the past quarter-century or so, is often much higher than measurements of C accumulation rates (CAR) obtained from in peat cores representing longer time periods (Ratcliffe et al., 2018; Liu et al., 2019). In contrast to modern C flux measurements, long-term measurements of CAR, derived from peat cores, typically span several millennia or more and thus are heavily weighted towards the period before industrialisation began (~1750 CE). Since industrialisation, there have been major changes to atmospheric

\* Corresponding author. School of Science and Environmental Research Institute, University of Waikato, Private Bag 3105, Hamilton, 3240, New Zealand.

E-mail address: [joss.ratcliffe@slu.se](mailto:joss.ratcliffe@slu.se) (J.L. Ratcliffe).

nitrogen (N) (Stevens et al., 2015) and phosphorus (P) deposition (Brahney et al., 2015; Wang et al., 2015b), and nutrient-mediated effects have been cited as hypothetical explanations for the discrepancy between long-term and modern records of peatland C uptake (Turunen et al., 2004; Yu, 2012; Ratcliffe et al., 2018).

Volcanoes are known to deliver pulses of nutrients to ecosystems (Delmelle et al., 2015; Stewart et al., 2020), including peatlands (Wolejko and Ito, 1986; Hughes et al., 2013). In oceans, so-called volcanic fertilisation can cause large drawdown of atmospheric CO<sub>2</sub> (Delmelle et al., 2015). In lakes, the deposition of tephra (volcanic ash) may impact diatom assemblages and sedimentation rates (Harper et al., 1986; Abella, 1988; Einarsson et al., 1993; Urrutia et al., 2007; Hutchinson et al., 2019). However, the influence of volcanically-derived nutrients on peatland carbon cycling has seldom been explored (Hughes et al., 2013). Volcanoes can deliver nutrients essential for plant growth, especially phosphorus, to ecosystems in three ways: (i) deposition of phosphatic compounds (presumably as PO<sub>4</sub><sup>3-</sup>) formed from P-bearing aerosols in turn derived from magmatic gases that are generated during eruptions; (ii) interaction of other acidic aerosols emitted during eruptions (including SO<sub>2</sub>, HCl, NH<sub>3</sub>, H<sub>2</sub>S, and HF; e.g. Roberts et al., 2019) with P-containing volcanic glass shards, pumice fragments, crystals (mineral grains), and lithics produced during the eruption; and (iii) by rapid dissolution of the particles of glass, pumice, and crystals, especially the phosphate-group mineral, apatite [Ca<sub>10</sub>(PO<sub>4</sub>)<sub>6</sub>(OH,F,Cl)<sub>2</sub>], after their deposition by enhanced acid-induced hydrolysis that results in the release of constituent elements/ions (e.g. Cronin et al., 2003; Mahowald et al., 2008; Delmelle et al., 2015).

Ombrotrophic (rain-fed) peatlands, by definition, receive nutrients solely from atmospheric deposition and are among the most nutrient-poor ecosystems in the world (Damman, 1986). However, the effect of nutrient enrichment on ecology and carbon cycling is often unknown. Low concentrations of nutrient inputs can greatly increase primary productivity (Aerts et al., 1992; Lund et al., 2009) but, at high nutrient loading, peatland plants can also exhibit signs of toxicity (Sheppard et al., 2011) and ultimately undergo competitive displacement (Limpens et al., 2003). In turn, such displacement could lead to loss of ecosystem function and reduced C sequestration associated with more nutrient-demanding plant communities (Gogo et al., 2011). Additionally, nutrient enrichment may enhance C losses by accelerating the microbial breakdown of peat (Bragazza et al., 2012). Recently, it has become increasingly clear that there have been major changes to global nutrient cycling which are capable of affecting even geographically remote locations (Neff et al., 2008; Brahney et al., 2015). For ecosystems located close to agricultural nutrient sources, such changes may be even more pronounced (Tipping et al., 2014).

Volcanoes are potentially an important source of nutrients for peatlands close to active volcanic centres, but few studies have considered the role of volcanic nutrient sources in mire ecology and biogeochemical cycling. In Iceland, deposition of volcanic dust is a major control on wetland ecology affecting bird and insect populations through bottom-up differences in ecosystem productivity (Gunnarsson et al., 2015), while in Japan, Wolejko and Ito (1986) coined the term “tephrotrophic” to describe mires affected by tephra deposition. These tephrotrophic mires, although ombrogenous in the sense that they received water only from rainfall, also maintain a rich fen-like plant community because of continued inputs of nutrients via tephra fall. Large areas of peatland in Te Ika-a-Māui, the North Island of Aotearoa New Zealand, are located close to recently active volcanic centres, both rhyolitic and andesitic in composition (Fig. 1; Wilson et al., 2009). Peatlands analogous to those described by Wolejko and Ito (1986) also exist in New Zealand, where oligotrophic vegetation has been unable to achieve dominance in mires proximal to Mt Taranaki, an andesitic

stratovolcano, due to continual fertilisation by frequent ash fall (McGlone et al., 1988; McGlone and Neall, 1994). Delivery of nutrients, especially phosphorus (P), into New Zealand peatlands during the Late Holocene is likely because of the presence of P (reported as P<sub>2</sub>O<sub>5</sub>) in both volcanic glass shards (Gehrels, 2009) and the presence of the phosphate-rich mineral apatite that has been identified in distal tephra deposits of the past c. 2000 years in the Waikato region, including in lakes, such as Lake Rotomanuka near Moanatuatua Bog, to the south of Hamilton (Fig. 1; Lowe, 1988). Additionally, the 1995–1996 andesitic eruptions of Mt Ruapehu in central North Island (Fig. 1) deposited fluorapatite, and analyses of tephra-samples (comprising mainly glass shards at distal sites) showed that P was present as a minor element (Cronin et al., 2003) (i.e., in quantities ≥ 0.1 wt%, following the quantitation terminology of Lowe et al., 2017). Similarly, distal tephra deposited in the Waikato region from the 1948 and 1975 andesitic eruptions of Mt Ngauruhoe contained P<sub>2</sub>O<sub>5</sub> in minor or trace amounts (Allen, 1948; Nelson, 1975; Gehrels, 2009).

Here we look at the effect of volcanic inputs on peatland carbon accumulation rates (CAR) by studying the Late Holocene section – the past c. 2000 years – of a large ombrogenous bog, Moanatuatua, in northern New Zealand in a temperate, humid climate and which has received accessions of tephra-fall deposits. This peatland, and another ~60 km to the north east (Kopuatai: Fig. 1), have been found to have high CO<sub>2</sub> uptake in the present day, and this uptake remains strong despite inter-annual climatic variation (Goodrich et al., 2017; Ratcliffe et al., 2019). Nutrient-related effects, associated with present-day land use, could offer an explanation for this elevated CO<sub>2</sub> uptake rate in both bogs. Both sites are strongly phosphorus limited as indicated from N:P ratios in plant foliage (Clarkson et al., 2005) although P limitation is weakening at Moanatuatua over time (Clarkson et al., 2020). In this paper, we examine peatland elemental accumulation rates, including C and elements relevant to growth, at a high chronological resolution to observe the effects on peatland elemental cycling.

We find that nutrient inputs, derived directly and indirectly from volcanic eruptions, have affected C cycling in the past, and therefore increased nutrient inputs could be primarily responsible for observed rapid C accumulation in peatlands where climatic limitations to growth are weak.

## 2. Methods and site description

### 2.1. Site description

The Scientific Reserve on Moanatuatua Bog is the remnant of a formally more extensive ombrotrophic peat bog (Fig. 1). The reserve's (natural) vegetation is dominated by *Empodisma robustum* (Restionaceae), growing in association with *Epacris pauciflora* (Ericaceae) and *Sporadanthus ferrugineus* (Restionaceae) (de Lange et al., 1999; Ratcliffe et al., 2020). In 1962 and again in 1972 two large fires broke out on the bog as the surrounding land was cleared for farming (Clarkson, 1997), and these fires were likely preceded by earlier burns also associated with land conversion (Reynolds, 1917; Cranwell, 1939). By 1979 the remaining Moanatuatua peatland was at its current size of ~140 ha (Matheson, 1979). The modern-day bog has undergone water table lowering and nutrient enrichment (Ratcliffe et al., 2020; Clarkson et al., 2020) but, despite this, the peat-forming community in the reserve persists and the site remains a strong sink for carbon (Ratcliffe et al., 2019).

### 2.2. Coring and core stratigraphy

The coring site (37.935970 S 175.366051 E), Moanatuatua south (Moa-south hereafter), was located 1.4 km south of a present-day

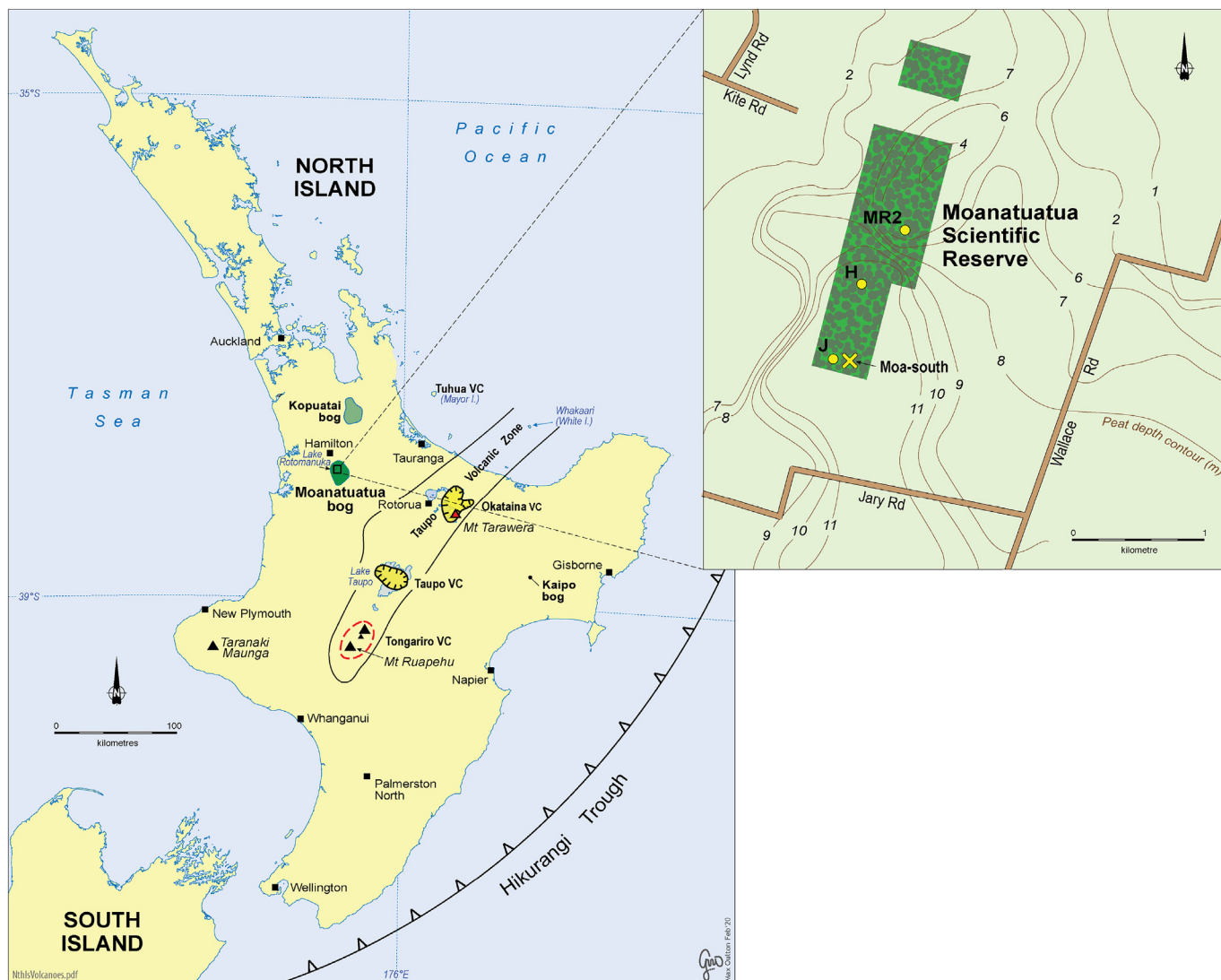


**Fig. 1.** Map of volcanoes and volcanic centres (VC) that have been active in North Island in the past c. 2000 years, including locations of the sources of tephras that were deposited in the upper part of Moanatuatua bog. The inset map (right) shows our coring site, Moa-south, on the Moanatuatua Scientific Reserve, and that of Gehrels (2009), namely MR2. Coring sites of Haenfling et al. (2017) (H) and Jara et al. (2017) (J) are also noted. Peat depths (in m) are from Davoren (1978).

CO<sub>2</sub> flux tower (Ratcliffe et al., 2019) and close to coring sites for a number of previous palaeoecological and palaeoclimatological studies (Haenfling et al., 2017; Jara et al., 2017; Newnham et al., 2019). A Russian corer, 10 cm in diameter, was used (Belokopytov and Beresnevich, 1955 in Jowsey, 1966), and two overlapping cores, taken less than 30 cm apart (and able to be easily connected using the tephra layers common to both), were transferred to PVC tubing in the field, and wrapped in cling film and stored horizontally and refrigerated prior to subsampling. We cored only 0.8 m of the deep peat column at the Moa-south coring site (Jara et al., 2017) as our intention was to study intensively an undisturbed sequence from the Late Holocene for which the volcanic eruption record and local climate are well understood. To supplement the findings we derived from our analyses of the Moa-south core, we also refer to cryptotephrostratigraphic work undertaken by Gehrels (2009), reported in Gehrels et al. (2010), on a matching core (MR2) taken from a location about 1 km from ours (Fig. 1).

The stratigraphies of the Moa-south and MR2 cores, correlated using tephrochronology, are shown in Fig. 2. Two visible rhyolitic tephras were identified in both cores: (1) Taupo Tephra, 2 cm thick,

erupted in  $232 \pm 10$  common era (CE) from Taupo Volcanic Centre (Hogg et al., 2012, 2019); and (2) Kaharoa Tephra, 5 cm thick, erupted in  $1314 \pm 12$  CE from Mt Tarawera (in the Okataina Volcanic Centre) (Hogg et al., 2003). Three cryptotephras (which are defined as glass shard and/or crystal concentrations too sparse to be visible to the naked eye as layers: Lowe, 2011) were identified in the peat in core MR2 by Gehrels (2009, 2010) as andesitic-dacitic members Tf4 (erupted c. 750 CE), Tf5 (erupted c. 1200 CE), and Tf6 (erupted c. 1250 CE) of the Mt Ruapehu-derived Tufa Trig Formation (Donoghue et al., 1997). They were identified (in MR2) by peaks in counts of brown glass shards (Supplementary Figure S1), the shards being characterised for major element compositions using methods reported in Gehrels et al. (2006). The approximate dates associated with the cryptotephras in MR2 are based on age data in Donoghue et al. (1997), Gehrels (2009), and Zawalna-Geer et al. (2016). It should be noted that, in common with other studies on cryptotephra glass-shard distribution that show the vertical spread of cryptotephra components in lake or peat deposits (Lowe, 2011; Pyne-O'Donnell, 2011), there is some uncertainty as to the exact horizons of deposition of TF5 and TF6, where the peaks in shards

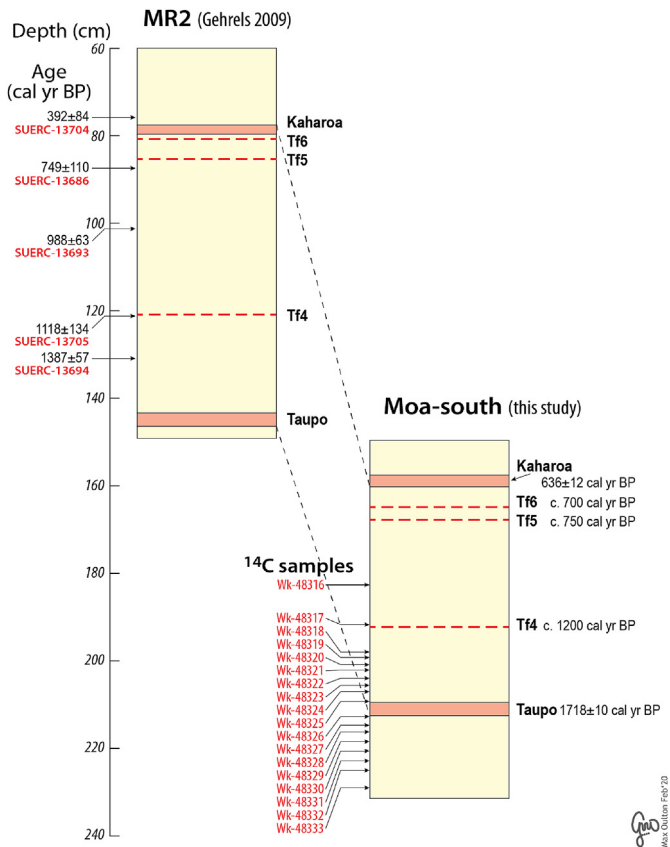


**Fig. 2.** Stratigraphy of Moanatuatua south core (Moa-south) and the corresponding section of core MR2 of Gehrels (2009). The two visible tephra linking the records are shown as orange bands; the three cryptotephra are depicted as red dashes. Calibrated radiocarbon ages (95% probability ranges) obtained for core MR2 are given (from Gehrels, 2009). Note there is some offset in depth between the two cores, see Shearer (1997) for more information on how tephra depth varies in Moanatuatua Bog. Sampling positions for radiocarbon ages obtained on the Moa-south core (this study) are also shown (see Table 1). SUERC = prefix for radiocarbon ages obtained at the NERC lab, Scotland; Wk = prefix for radiocarbon ages obtained at the Waikato lab, Hamilton, New Zealand. (For interpretation of the references to colour in this figure legend, the reader is referred to the Web version of this article.)

were not pronounced, and there was a relatively wide distribution of shards over a ~10 cm interval Gehrels (2009, 2010).

### 2.3. Bulk density

Bulk density was measured continuously at 1-cm vertical resolution, with volume calculated using the water displacement technique (Chambers et al., 2011) and then the dry weight was measured after drying the samples at 55 °C until at a constant weight was attained.

### 2.4. C/N

Samples were oven-dried at 55 °C and homogenised using a steel-ball mill which was cleaned and dried between samples to avoid contamination. Dried peat with a mass of 0.02 g was weighed out and analysed for C and N content using a Vario El cube CHNOS Elemental Analyzer (Elementar Analysensysteme GmbH, Hanau, Germany), with a precision of ±0.1% as determined from acetanilide standards.

### 2.5. Elemental analysis by inductively coupled plasma-mass spectrometry (ICP-MS)

In order to study the effect of volcanism on the peatland, we analysed the peat for geochemical markers signifying the input of volcanic material and volcanically derived phosphorus. The core was subsampled for ICP-MS analysis at 1-cm intervals. Care was taken to avoid contamination and sample preparation was carried out in a random order to limit the possibility of false trends appearing as a result of contamination. Dried samples were coarsely homogenised by hand, with the steel-ball mill only being used to prepare samples for C/N analysis, and 0.5 g of dried sample was ashed at 450 °C for 4 h following Yafa and Farmer (2006). One ml of concentrated nitric acid was added to the ash and samples were digested on a heat block at 80 °C for 2 h. Samples were made up to 50 ml with de-ionized water and centrifuged at 1800 rpm for 10 min. Ten ml of the sample was then decanted and used for ICP-MS analysis of 16 elements: Mg, Al, P, S, K, Ca, Cr, Co, Cu, Sr, Ba, Pb and U. Also analysed were Hg, Fe, and Ni but the results for these are considered less reliable due to volatilisation (Hg) (Yafa and Farmer, 2006) and potential contamination from the sampling and laboratory process (Fe and Ni). The elements discussed in detail (P, Cu, Pb) are known not affected by ashing at 450 °C (Yafa and Farmer, 2006). Little or no information exists as to the volatilisation of U in peats, but the ashing method has been applied to peats previously and U is assumed not to be lost (Marx et al., 2009). It is worth noting that the acid digestion procedure may mobilise some elements from the tephra material (Blockley et al., 2005), but strong acids or bases are usually necessary to fully dissolve the peat matrix and are commonly used to prepare shards for geochemical analysis and do not alter the shard geochemistry of rhyolitic tephra in any detectable way (Roland et al., 2015). Moreover, the glass analyses reported on glass from Moanatuatua Bog (see Table 3 below) show high original analytical totals, ≥97%, suggesting that the glass shards have not been compromised geochemically via pretreatment (e.g. Hunt and Hill, 1993; Pearce et al., 2014; Lowe et al., 2017). Additionally both the peatland itself and the eruptive condensates associated with the eruptions (Óskarsson, 1980) may be highly acidic. Analyses were undertaken using an Agilent 8900 ICP-MS (Agilent Technologies, Santa Clara, USA) controlled by MassHunter Workstation (version 4.5). Sample introduction occurred via an SPS4 autosampler (Agilent Technologies, Santa Clara, California, USA) and PVC tubing (Pulse Instrumentation, Mequon, Wisconsin, USA). A 0.05–0.1 mL/min micromist U-Series nebuliser (Glass Expansion, Melbourne, Australia) was attached to a quartz Scott Type spray chamber followed by a quartz torch with 2.0 mm injector (Agilent Technologies, Santa Clara, USA). Following the plasma, the sample was introduced to the rest of the instrument via a nickel sampler and skimmer cone, followed by an extraction omega lens (Agilent Technologies, Santa Clara, USA). The ICP-MS was optimized to maximum sensitivity ensuring oxides and doubly-charged ions were less than 2%.

An internal standard consisting of Sc, Ge, Rh, Te, and Ir was utilised to correct for instrumental drift. Standards were analysed every 20 samples and re-calibration was performed every 100 samples. Blank samples were analysed every 10 samples to ensure minimal carryover between samples. Instrument detection limits were as follows: 1.2 µg/L Mg, 5.3 µg/L Al, 22 µg/L Ca, 73 µg/L S, 6.4 µg/L K, 0.023 µg/L Cr, 1.0 µg/L Fe, 0.035 µg/L Co, 0.027 µg/L Cu, 0.0087 µg/L Sr, 0.069 µg/L Ba, 0.017 µg/L Pb, 0.0046 µg/L U. Average blank concentrations ( $n = 19$ ) were as follows: 1.2 µg/L Mg, 6.2 µg/L

Al, < DL Ca, 190 µg/L S, < DL K, 0.004 µg/L Cr, 4.8 µg/L Fe, < DL Co, 0.003 µg/L Cu, 0.001 µg/L Sr, 0.01 µg/L Ba, < DL Pb, < DL U. Sample reproducibility, as measured using relative standard deviations (RSD), was <5%. Spiked samples were used to determine digestion efficiency as a standard reference material was unavailable at the time. Spike recoveries ranged from 80.3 to 102% with RSDs ranging from 3.1 to 8.7%.

## 2.6. Chronology and age-depth model for Moa-south core

### 2.6.1. Radiocarbon samples

Subsamples of wet peat (Fig. 2) were disaggregated using the hot NaOH method (Mauquoy et al., 2010) and sieved at 120 µm, discarding the filtrate. Above-ground material, mainly plant stems and charcoal, was manually separated under a microscope and was cleaned using de-ionized water. Combinations of macroscopic charcoal, *Empodisma* stems with visible stomata, and wood was used for radiocarbon (<sup>14</sup>C) dating (Table 1, Fig. 2). Material for dating was stored in de-ionized water, mildly acidified with H<sub>2</sub>SO<sub>4</sub> to preserve the samples, and then submitted to the Waikato Radiocarbon Dating Laboratory for accelerator mass spectrometry (AMS) dating, using the Keck Carbon Cycle Accelerator Mass Spectrometer facility at the University of California, Irvine, USA. It is important to use surface samples for dating as both *E. robustum* and *S. ferrugineus* have deep anchor roots which can extend several metres into the peat (Clarkson et al., 2009).

### 2.6.2. Age-depth model

Calibrated <sup>14</sup>C ages were combined with the high-precision dates for the two visible tephra layers, Kaharoa Tephra at 158 cm depth (1314 ± 12 CE), and Taupo Tephra at 210 cm depth (232 ± 10 CE) (Fig. 2). The tephra layers were readily identified in the field by their distinctive physical properties and their stratigraphic superpositions in the core near the bog surface. Both have been well characterised or 'fingerprinted' previously in studies on numerous lakes and bogs in the Waikato region using their ferromagnesian mineralogical assemblages and glass-shard major element compositions, including in Moanatuatua Bog itself as reported by

Gehrels (2009) and Newnham et al. (2019) (see also Green and Lowe, 1985; Lowe, 1988; de Lange and Lowe, 1990; Hodder et al., 1991; Gehrels et al., 2006). The newly acquired <sup>14</sup>C dates are consistent with the identifications. The lowest C content of the peat was used to indicate the specific point (instant in time) at which the tephra layers were deposited, with 16.9% C at 158 cm and 19.9% C at 210 cm, compared to the core average of 47.1% (Table 2). The age-depth model was constructed using the Bayesian software BACON 3.3.3 (Blaauw and Christen, 2011) modelled against SHCal13 of Hogg et al. (2013). The prior accumulation rate was set at 10 yr cm<sup>-1</sup> and a 1-cm section depth was specified, and the default sample size was increased to 14,000 to obtain a satisfactory mix of 1000 Markov Chain Monte Carlo iterations. Other accumulation and memory priors were set to the default values following Goring et al. (2012).

## 2.7. C accumulation rates

C accumulation rates were calculated using the measured carbon content of each 1-cm slice divided by the modelled age difference between the top and bottom of the slice, produced using the age-depth model, with the final rate converted to a per-square-metre basis and presented as g C m<sup>-2</sup> yr<sup>-1</sup>.

## 3. Results

### 3.1. Chronology and age-depth model

All dates were included in the initial age-depth model but the optimal model did not pass through dates Wk-48328 and Wk-48329, which were identified as outliers, and so were not included in the final model. BACON is designed to infer periods when a hiatus in the sequence is likely to have occurred, with short hiatuses being progressively more likely. However, despite a period of slow peat accumulation at 187–191 cm depth, no hiatus was detected, i.e. the slow accumulation rate was plausible. The model displayed considerable variation in the peat accumulation rate (Table 2), most notably with periods of rapid accumulation at depths of 207–220 cm and 150–161 cm.

**Table 1**

Radiocarbon ages used to construct the chronology for the Moanatuatua south core (see also Fig. 2).

Laboratory no. (Waikato)	Depth (cm)	Macrofossils selected for AMS dating	Conventional radiocarbon age ( <sup>14</sup> C yrs BP ± 1σ)	'Best estimate' weighted mean age/date (CE) <sup>b</sup>	2σ calibrated date range (CE)
Wk48316	182	<i>Empodisma</i> stem	1035 ± 15	1039	916–1122
Wk48317	191	Macro charcoal <sup>a</sup>	1562 ± 19	592	490–591
Wk48318	197	Macro charcoal	1677 ± 19	431	383–489
Wk48319	198.5	Macro charcoal	1668 ± 19	399	365–440
Wk48320	201	Macro charcoal	1737 ± 19	366	336–399
Wk48321	202	Macro charcoal	1832 ± 19	349	325–377
Wk48322	204	Macro charcoal	1792 ± 19	315	283–347
Wk48323	206	Macro charcoal	1790 ± 19	292	252–292
Wk48324	208	Macro charcoal	1815 ± 20	280	244–310
Wk48325	209.5	Macro charcoal	1782 ± 20	267	231–301
Wk48326	211.5	<i>Empodisma</i> stem	1678 ± 14	259	229–294
Wk48327	214	Wood with external bark	1864 ± 16	251	218–283
Wk48328 <sup>c</sup>	215.5	<i>Empodisma</i> stem	1480 ± 15	244	204–274
Wk48329 <sup>c</sup>	218	<i>Empodisma</i> stem	1689 ± 14	238	183–264
Wk48330	220	<i>Empodisma</i> stem	1838 ± 15	232	162–257
Wk48331	222	<i>Empodisma</i> stem	1654 ± 14	211	151–236
Wk48332	224	<i>Empodisma</i> stem	1888 ± 14	190	134–228
Wk48333	228.5	<i>Empodisma</i> stem	1962 ± 15	110	60–188

<sup>a</sup> Macro = >120 µm.

<sup>b</sup> The weighted mean age (or date in this case) is a single-age representation that takes into account the general outcome of all MCMC iterations in the Bacon modelling (Blaauw and Christen, 2011).

<sup>c</sup> These dates were identified as outliers and rejected from the BACON modelling (Fig. 3).

**Table 2**  
Summary of peat carbon and phosphorus accumulation rates, ratios of C:P and N:P, and measurements of bulk density and C content. Data in full are reported in [Supplementary Figure S2](#).

Zone	Depth range (cm)	Date range (95% prob) CE	Bulk density g cm <sup>-3</sup>	Carbon accumulation rate g C cm yr <sup>-1</sup>	Phosphorus accumulation rate g P cm yr <sup>-1</sup>	C %	C:P	N:P	n
Z6	160–150	1210–1400	0.109 ± 0.015	83 ± 20	0.031 ± 0.004	34 ± 10	2704 ± 556	83 ± 22	11
Z5	185–161	990–1290	0.076 ± 0.007	35 ± 7	0.010 ± 0.003	54 ± 6	3550 ± 383	97 ± 14	25
Z4	195–186	390–990	0.071 ± 0.008	8 ± 3	0.003 ± 0.001	54 ± 1	3436 ± 433	96 ± 14	10
Z3	204–196	280–520	0.090 ± 0.018	24 ± 6	0.001 ± 0.002	46 ± 6	3663 ± 765	104 ± 19	9
Z2	221–205	160–340	0.093 ± 0.019	86 ± 44	0.026 ± 0.012	41 ± 9	3374 ± 608	96 ± 16	17
Z1	230–222	120–230	0.089 ± 0.005	34 ± 9	0.001 ± 0.003	51 ± 1	4153 ± 798	122 ± 25	9
All	230–150	120–1400	0.087 ± 0.018	48 ± 36	0.015 ± 0.012	47 ± 9	3448 ± 659	98 ± 19	81

### 3.2. Carbon accumulation rate and changes in physical and chemical properties in the Moa-south core

The CAR of the Moa-south core (Fig. 4) was found to vary considerably across the 1200-year-long time period considered.

We defined six zones within which the CAR was relatively consistent (Table 2) and describe these in the following section. Bulk density, % C, % N and C:N ratios are presented in full in [Supplementary Figure S2](#).

#### 3.2.1. Zone 1 (230 cm–222 cm, 120 to 230 CE)

Zone one begins at the base of the sequence cored, 15 cm below the Taupo Tephra. Bulk density is close to the core average, varying between 0.08 and 0.1 g cm<sup>-3</sup> and % C is high, and steady, between 49% and 51% indicating a low mineral content of the peat. CAR in this zone is variable starting at 28 g C m<sup>-2</sup> yr<sup>-1</sup> and rising to 44 g C

m<sup>-2</sup> yr<sup>-1</sup> reflecting an increase in the sedimentation rate. The C:P and N:P ratios start very high, at 5560 and 170, respectively, and these decline to 4000 and 110, respectively, at the end of the zone.

#### 3.2.2. Zone 2 (221 cm–205 cm, 160 to 340 CE)

Zone two begins 6 cm below the Taupo Tephra. Bulk density in this zone reaches the peak value for the core, 0.13 g cm<sup>-3</sup>, rising and fluctuating in the first 10 cm before reaching a peak at 210 cm and plateauing at the end of the zone. Carbon content clearly shows the influence of the Taupo Tephra with a sharp drop from 50% C down to 42% C at 215 cm and a further drop to 20% C matching the rise in bulk density at 210 cm. The CAR for this zone is greatly elevated, increasing to between 140 and 160 g C m<sup>-2</sup> yr<sup>-1</sup> at the start of the zone, briefly dropping to 25 g C m<sup>-2</sup> yr<sup>-1</sup> at the peak of tephra-derived glass shard abundance, but otherwise remaining elevated above 70 g C m<sup>-2</sup> yr<sup>-1</sup> to the end of the zone.

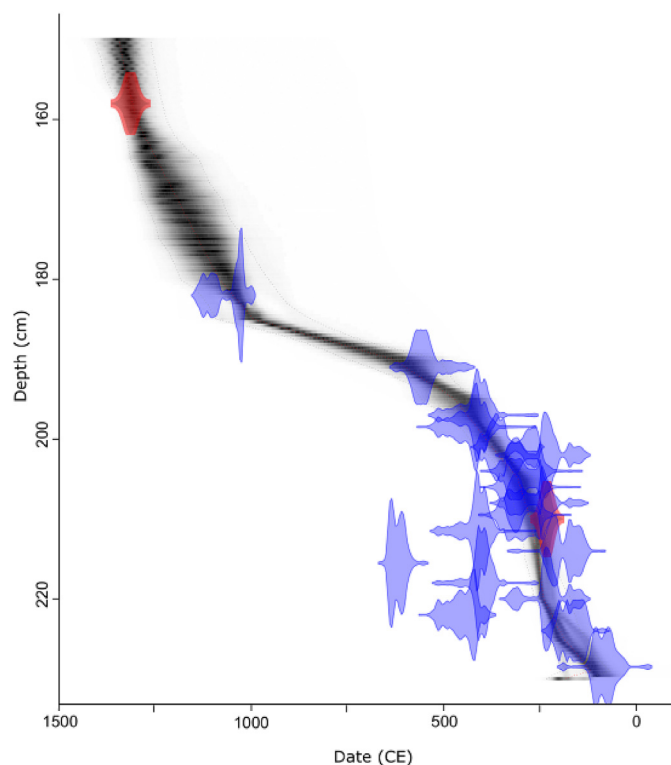


**Fig. 3.** Age-depth model (in calendar years plotted as dates) for the core produced using Bayesian modelling via BACON (Blaauw and Christen, 2011), and 14C ages as listed in Table 1. Dates adopted for the two visible tephra (red shapes) are Taupo, 232 ± 10 CE (Hogg et al., 2012, 2019), and Kaharoa, 1314 ± 12 CE (Hogg et al., 2003). Blue shapes represent the statistical probability of age/depth associated with each date, and the back/grey shading represents the 95% confidence interval of the preferred age/depth model. (For interpretation of the references to colour in this figure legend, the reader is referred to the Web version of this article.)

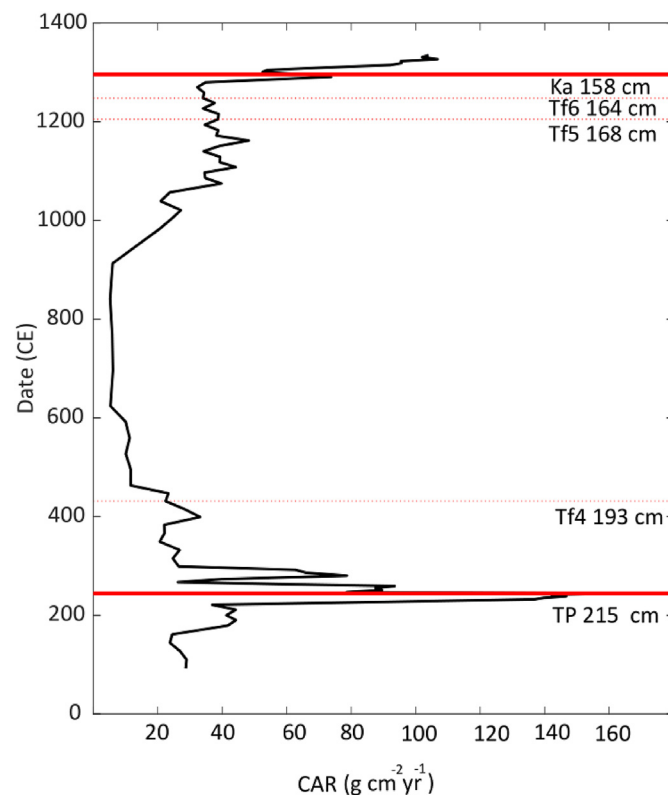


**Fig. 4.** Carbon accumulation rate (CAR) plotted against calendar date and depth in Moa-south core. The isochrons provided by the Taupo (TP) and Kaharoa (KA) tephra are represented by the two red solid horizontal lines, and the inferred positions of the Tufa Trig cryptotephra (Tf4–6) are marked by dotted lines. (For interpretation of the references to colour in this figure legend, the reader is referred to the Web version of this article.)

### 3.2.3. Zone 3 (204 cm–196 cm, 280 to 520 CE)

Zone three is still affected by the Taupo eruption and possibly the smaller TF eruptions, and there is a rapid decline in bulk density from  $0.12 \text{ g cm}^{-3}$  to  $0.07 \text{ g cm}^{-3}$  mirroring an increase in C content from 35% at the start of the zone to 53% at the end. CAR is consistently between 20 and  $27 \text{ g C m}^{-2} \text{ yr}^{-1}$ , except a peak between 200 cm and 197 cm where CAR increased to  $33 \text{ g C m}^{-2} \text{ yr}^{-1}$  at 199 cm, essentially matching the inferred location (in corresponding core MR2 of Gehrels, 2009) of cryptotephra Tf4 at 197 cm (Fig. 4), and the large spikes in U, Cu, and Pb concentrations also at 197 cm depth (Fig. 5).

### 3.2.4. Zone 4 (195 cm–186 cm, 390 to 990 CE)

Zone four contains the lowest bulk density values found in the core, between  $0.06$  and  $0.08 \text{ g cm}^{-3}$ , the C content of the peat is high and consistent at 50% or more, also consistent with the low shard count in this section inferred from the MR2 core, implying minimal volcanic activity (Supplementary Figure S1). During this period, CAR was at its lowest, varying between  $13 \text{ g C m}^{-2} \text{ yr}^{-1}$  and  $5 \text{ g C m}^{-2} \text{ yr}^{-1}$  (Fig. 4).

### 3.2.5. Zone 5 (185 cm–161 cm, 840 to 1320 CE)

Zone five had low and steady bulk density between  $0.06$  and  $0.09 \text{ g cm}^{-3}$  and a high and consistent % C, much like Zone 4 preceding it. Unlike Zone four, however, the shard count, inferred from the MR2 core (Supplementary Figure S1) is greater in this section and Al, Cu, Pb, and U accumulation and concentration (Supplementary Figure S3) are elevated. The CAR was found to increase steadily, varying between 20 and  $49 \text{ g C m}^{-2} \text{ yr}^{-1}$  (Fig. 4).

### 3.2.6. Zone 6 (160 cm–150 cm, 1210 to 1400 CE)

Zone six is marked by a rapid increase in bulk density, up to  $0.12 \text{ g cm}^{-3}$ , corresponding with a decline in C content down to 17% and the presence of the Kaharoa Tephra. CAR varies between 73 and  $107 \text{ g C m}^{-2} \text{ yr}^{-1}$ , and, as with the Taupo Tephra in Zone 2, there is a small dip in CAR, to  $52 \text{ g C m}^{-2} \text{ yr}^{-1}$ , which corresponds with peak glass-shard deposition (Fig. 4). This zone is also characterised by the highest accumulation rates for of Al, Cu, Pb, and U seen in the record (Fig. 5) and the lowest C:P and N:P ratios (Fig. 6).

## 3.3. Carbon accumulation rate and elemental concentrations

ICP-MS analyses of elements resulted in counts above the detection limit for almost all elements considered, except for silver and cadmium for which approximately half the analyses were below the detection limit and mercury was consistently below the detection limit, as would be expected due to volatilisation after ashing (Yafa and Farmer, 2006). The results of the analyses are presented in full in the Supplementary Data. In order to investigate how these elements varied with CAR, we performed linear regressions between all the elements we had measured and the CAR (Fig. 7). The elements with the greatest correlation, Al, U, Pb, and Cu were then plotted against CAR (Fig. 5). Elements including Al, Pb, U, Cu, Cr, Co and K correlated positively with CAR whereas Ba, Ca, Sr, and Mg correlated negatively and, in the cases of Ca, Sr and Mg, their correlations were quite strong.

## 3.4. Carbon, nitrogen, and phosphorus accumulation rates and stoichiometric ratios

Carbon, nitrogen, and phosphorus accumulation rates followed a similar pattern to each other and were highly correlated (Figs. 8 and 9), maintaining consistent stoichiometric ranges throughout most of the time series (C:P of 3500 and P:N of 80), with the exception of the two visible-tephra depositional events (Taupo and Kaharoa), and the short period at the very start of the sequence between ~90 and ~220 CE. Carbon-to-phosphorus ratios were at their highest in the earliest part of the time series, around 4000, then declined greatly with the deposition of the Taupo Tephra to around 3300 before increasing and stabilising to 3500, and then declining again to around 2700 at the time of deposition of the Kaharoa Tephra (Fig. 8).

Rates of C accumulation varied from  $160 \text{ g C m}^{-2} \text{ yr}^{-1}$  at ~244 CE (216 cm depth) to  $5.2 \text{ g C m}^{-2} \text{ yr}^{-1}$  at ~840 CE (187 cm depth). Extremes in CAR were mirrored by those of P,  $0.04 \text{ g C m}^{-2} \text{ yr}^{-1}$  at ~244 CE (216 cm depth) and  $0.001 \text{ g C m}^{-2} \text{ yr}^{-1}$  at 627 CE (190 cm depth) (Fig. 8), and also N accumulation rate of  $4.0 \text{ g C m}^{-2} \text{ yr}^{-1}$  at ~244 CE (216 cm depth) and  $0.1 \text{ g C m}^{-2} \text{ yr}^{-1}$  at ~840 CE (187 cm depth) (Fig. 8).

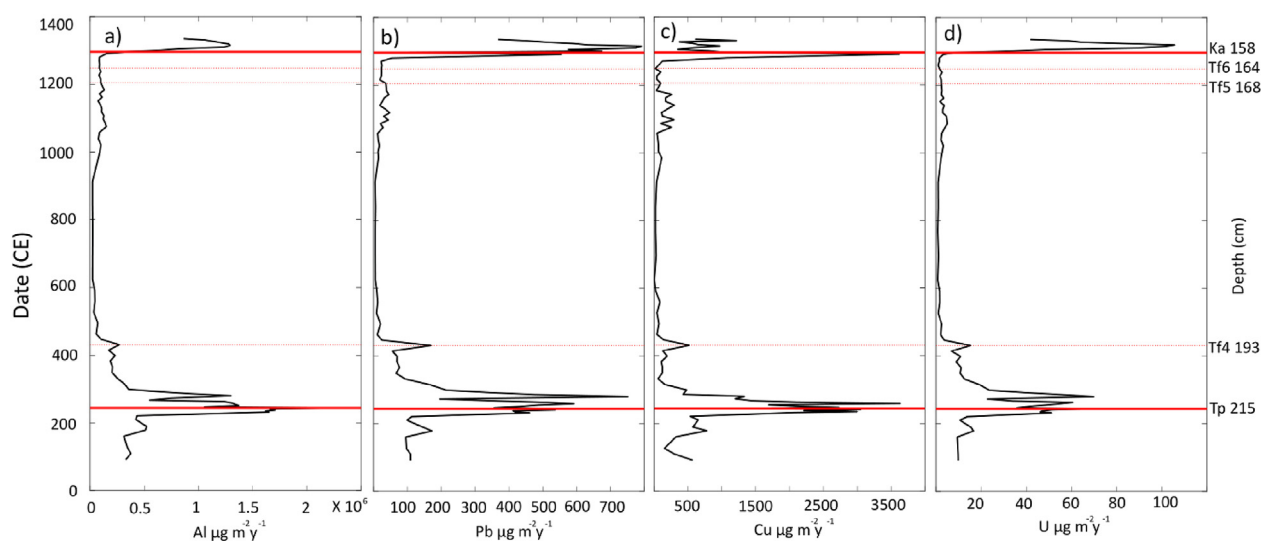


**Fig. 5.** (a) Aluminium (Al), (b) Lead (Pb), (c) copper (Cu), and (d) Uranium (U) accumulation rates plotted against age (date in calendar years). Tephra or cryptotephra deposits are shown as solid or dashed horizontal lines, respectively, as described in Fig. 4 and the names and depth of these tephra have been added as annotations.

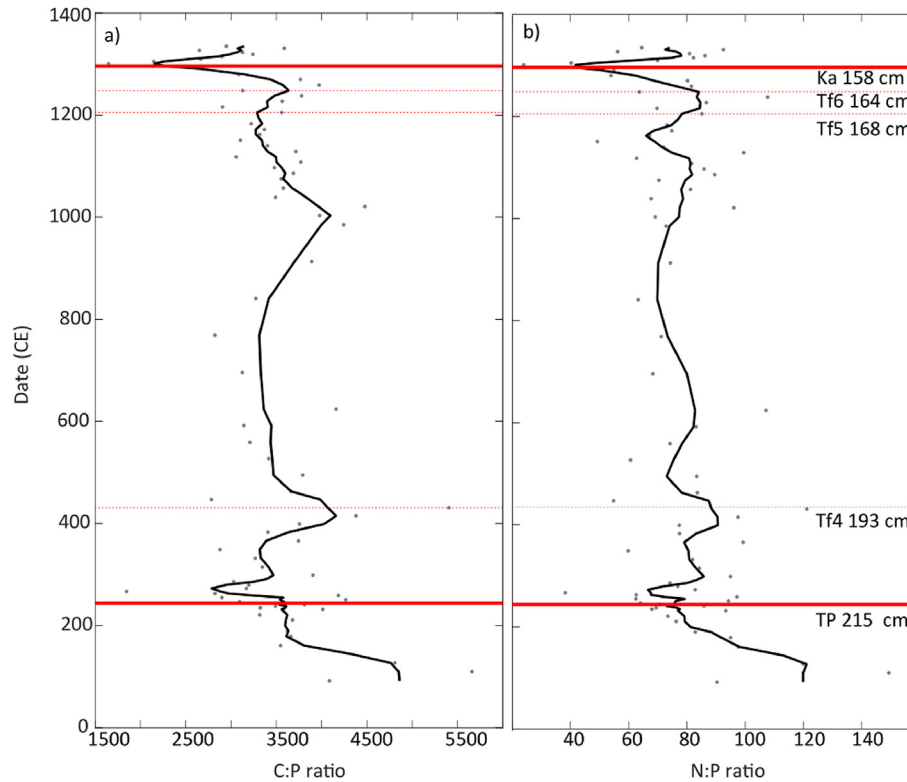


**Fig. 6.** (a) C:P ratio plotted as points, with a ten-sample moving mean plotted as a line; (b) N:P ratio plotted as points, against age (date in calendar years), with a ten-sample moving mean plotted as a line. Tephra or cryptotephra deposits are shown as solid or dashed horizontal lines, respectively, as described in Fig. 4 and the names and depth of these tephra have been added as annotations.

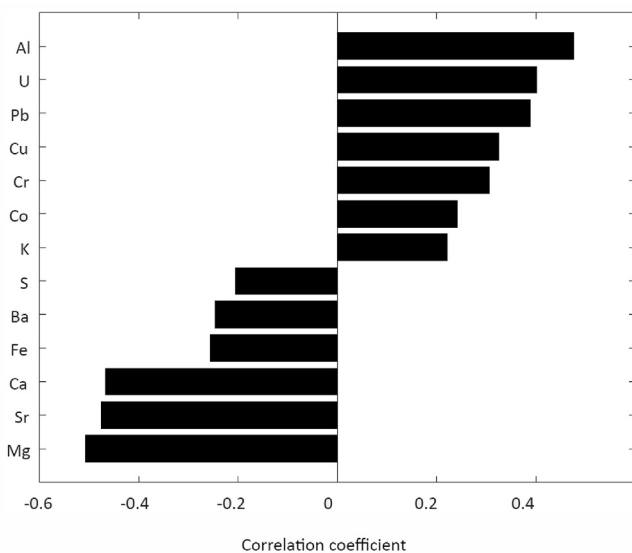


**Fig. 7.** Correlation coefficients of CAR and elemental concentrations for linear regressions where  $P < 0.05$ .

### 3.5. Correlations between C, N, and P accumulation rates

Carbon accumulation rates were found to have a strong positive linear correlation with N ( $R^2$  0.98) and P ( $R^2$  0.91) accumulation rates (Fig. 9), and this was most pronounced in the lower, 'typical' range of CAR 0–60  $\text{g C m}^{-2} \text{yr}^{-1}$ , with greater residuals at high CAR  $> 60 \text{ g C m}^{-2} \text{yr}^{-1}$ .

## 4. Discussion

Carbon accumulation rates were found to be elevated following the deposition of two visible rhyolitic tephra layers, Taupo (Tp) ( $232 \pm 10 \text{ CE}$ ) and Kaharoa (Ka) ( $1314 \pm 12 \text{ CE}$ ), both containing phosphorus as a minor element in constituent glass shards (Table 3) and also in apatite crystals (further potential sources of P are discussed further below). The CAR increased from a background of  $23.1 \text{ g C m}^{-2} \text{yr}^{-1}$  (Table 2), comparable to that for other southern hemisphere peatlands (Yu, 2011), to a maximum sustained rate of  $110 \text{ g C m}^{-2} \text{yr}^{-1}$  after Tp and  $84 \text{ g C m}^{-2} \text{yr}^{-1}$  after Ka. The CAR following the Tp and Ka tephra is more typical of rates for contemporary peatland  $\text{CO}_2$  uptake – for example, a rate of  $74 \text{ g C m}^{-2} \text{yr}^{-1}$  was calculated from 24 site-years across six peatlands by Lu et al. (2017).

Additionally, a small increase in CAR, to 30–35  $\text{g C m}^{-2} \text{yr}^{-1}$ , was evident at c. 420 CE, with concurrent spikes in uranium, lead, and copper (Fig. 5). This increase may relate to the deposition of the dacitic Tufa Trig tephra, Tf4, derived from Mt Ruapehu (Donoghue et al., 1997), identified as a cryptotephra in core MR2 in Moana-tuatua Bog by Gehrels (2009) (Fig. 2; Table 3). Possible increases in CAR were also evident in Zone 5 in which the closely-spaced andesitic-dacitic Tufa Trig tephra Tf5 and Tf6 (aged c. 1200 and c. 1250 CE, respectively) were identified in nearby core MR2 (Fig. 2; Table 3).

Carbon accumulation rate has rarely been measured in peatlands across time periods spanning tephra deposition events, with the only other example of which we are aware being reported for a bog in Hokkaido, Japan (Hughes et al., 2013), where CAR above  $100 \text{ g C m}^{-2} \text{yr}^{-1}$  occurred after deposition of a rhyolitic tephra (B–Tm) erupted from Changbaishan (or Baitoushan) volcano located more than 1000 km away on the China/North Korea border.

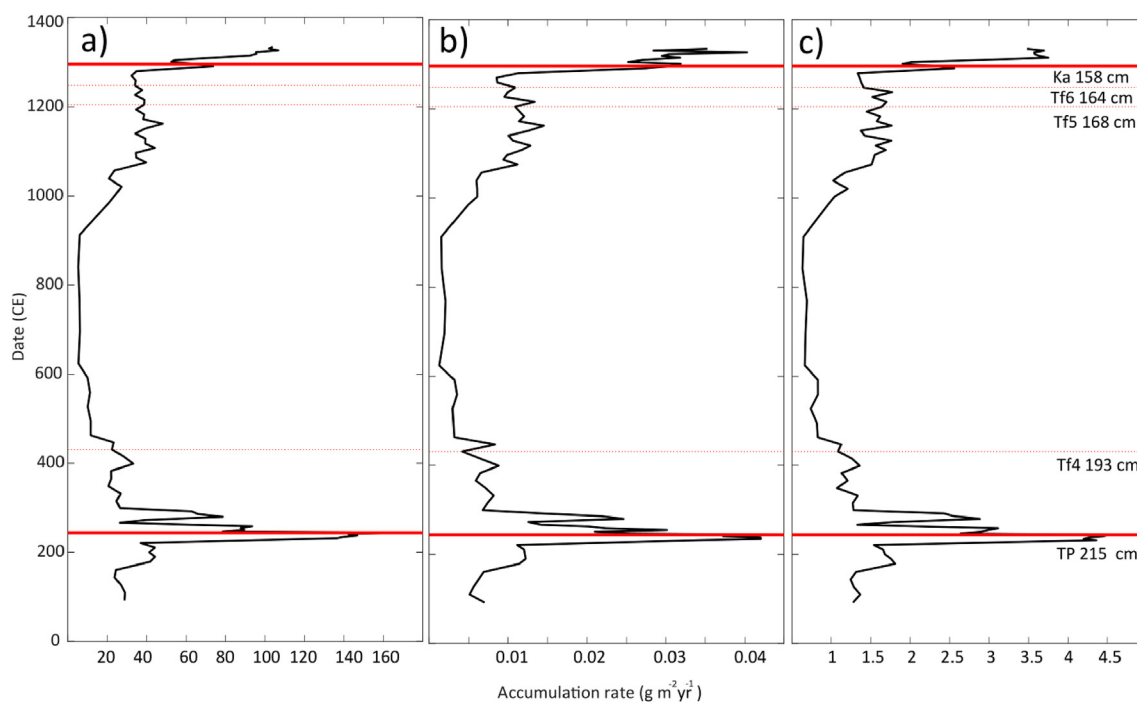


**Fig. 8.** Elemental carbon accumulation (a), phosphorus accumulation (b), and nitrogen accumulation (c), each plotted against age (date in calendar years) and depth. Tephra or cryptotephra deposits are shown as solid or dashed horizontal lines, respectively, as described in Fig. 4.

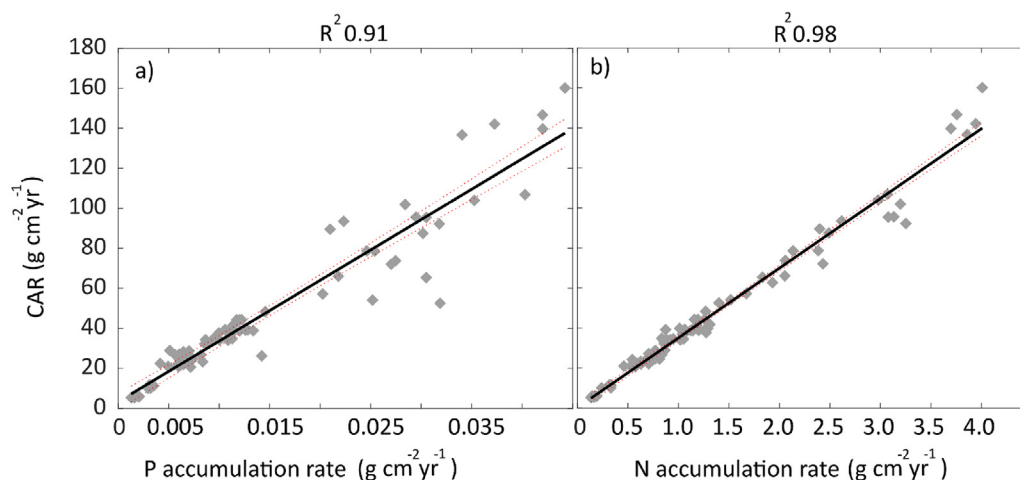


**Fig. 9.** (a) Linear regression of elemental P accumulation rate and C accumulation rate (CAR); (b) Linear regression of elemental N accumulation rate and C accumulation rate.

In that case, elevated CAR, linked to P inputs, was found to be sustained for about 300 years rather than the ~80 years we found here, but this apparent extended period could be, in part, due to coarser dating resolution used by Hughes et al. (2013). The rapid CAR we found here, and that in Hughes et al. (2013), would be unlikely to be detected in typical paleoecological studies with around one date per 1000 years (Payne et al., 2016). Therefore, we do not consider the paucity of examples in the literature to preclude this phenomenon from being more widespread.

Modern experiments and palaeoecological reconstructions suggest that the impacts of tephra on peatland plant mortality can be inconsistent (Payne and Blackford, 2008, 2005). Vascular plants can remain unaffected by tephra falls up to 6 cm thick (Hotes et al., 2006). Much thicker deposits than reported here for Moanatuatua – for example, a 22-cm thick tephra layer in the montane Kaipo bog

in New Zealand (Fig. 1) – may cause disruption of the plant community (Giles, 1999). Beyond the immediate disturbance effect, the nutrient impact may be of greater importance for CAR. Phosphorus is one of the key limiting nutrients in ombrotrophic peatlands (Aerts et al., 1992; Clarkson et al., 2005), with inputs coming solely from atmospheric inputs, both direct and indirect via rapid weathering of atmospheric dust.

The fallout from two Late Holocene volcanic eruptions in North Island, including the Taupo event, have been previously associated with increased lake primary productivity at a distal site (Lake Poukawa) in Hawke's Bay (Fig. 1), and the authors concluded this enhancement was likely to be driven by P (Harper et al., 1986). Our data, involving five tephra/cryptotephra deposits, also indicate that increased P input is likely to be the mechanism behind the increase in C accumulation. This mechanistic explanation is evident from the

**Table 3**  
Oxide contents of volcanic glass shards, expressed as mean weight percent ( $\pm 1$  sd), derived by electron microprobe analysis of glass from tephra and cryptotephra in core MR2<sup>a</sup>.

Tephra	SiO <sub>2</sub>	Al <sub>2</sub> O	TiO <sub>2</sub>	FeO <sup>b</sup>	MnO	MgO	CaO	Na <sub>2</sub> O	K <sub>2</sub> O	P <sub>2</sub> O <sub>5</sub>	H <sub>2</sub> O <sup>c</sup>	n
Kaharoa	77.78 (2.27)	12.13 (1.17)	0.09 (0.14)	0.8 (0.73)	0.05 (0.05)	0.08 (0.25)	0.44 (0.74)	4.18 (0.42)	4.11 (0.43)	0.00 (0.04)	1.11 (0.96)	71
Tf6	63.09 (0.39)	14.46 (0.28)	1.12 (0.11)	6.52 (0.25)	0.12 (0.11)	2.07 (0.22)	4.93 (0.26)	3.78 (0.22)	2.79 (0.20)	0.25 (0.08)	1.37 (0.29)	22
Tf5	68.34 (1.77)	13.53 (1.15)	1.03 (0.16)	5.29 (0.94)	0.11 (0.06)	1.18 (0.31)	3.60 (1.03)	3.7 (0.24)	3.03 (0.81)	0.23 (0.05)	1.21 (0.37)	17
Tf4	66.38 (2.14)	14.61 (1.99)	0.92 (0.12)	4.58 (0.99)	0.07 (0.08)	1.06 (0.44)	3.70 (1.74)	4.05 (0.30)	3.32 (1.42)	0.20 (0.03)	2.04 (0.49)	6
Taupo <sup>d</sup>	75.69 (0.82)	12.77 (0.29)	0.25 (0.06)	1.90 (0.30)	0.10 (0.07)	0.25 (0.06)	1.52 (0.19)	4.26 (0.31)	2.93 (0.37)	0.03 (0.02)	3.08 (1.52)	61

n, number of individual shards analysed in generating the mean.

<sup>a</sup> Data (normalised to 100% loss-free basis) are from [Gehrels \(2009\)](#). Analyses were acquired at the NERC Tephra Analytical Unit, University of Edinburgh, in February and June 2007. Mean values for independently characterised laboratory standards, TB1G and Lipari, are available in [Newnham et al. \(2018\)](#).

<sup>b</sup> Total Fe expressed as FeO.

<sup>c</sup> 'Water' by the difference between the original analytical total and 100.

<sup>d</sup> Further electron microprobe analyses on glass from Taupo Tephra in Moanatuatua Bog are reported by [Newnham et al. \(2019, p. 384\)](#).

stoichiometric ratios, which shifted towards greater P relative to C and greater P relative to N at the time of deposition of Tp and Ka tephra, and also at close to the inferred times of deposition of cryptotephra Tf4, Tf5, and Tf6 ([Fig. 9](#)). Although we did not find evidence of a change in absolute (numerical) P concentration, such a change is not unexpected given that P is rapidly utilised and recycled by peatland plants within the shallow surface layers of bogs, moving up vertically through the peat ([Wang et al., 2014](#)). Because of rapid re-cycling within the peatland ecosystem, P accumulation rate is considered a more reliable indicator of P inputs than P concentration ([Wang et al., 2015a](#)). It was initially speculated that there would be a net loss of P from ombrotrophic bogs over time ([Walbridge and Navaratnam, 2006](#)) but this has subsequently been shown not to be the case, with bogs displaying net P accumulation very close to P inputs ([Wang et al., 2015a](#); [Schillereff et al., 2016](#); [Worrall et al., 2016](#)). Moanatuatua is no exception to this, with a rate of P accumulation almost identical to the assumed long-term rate of P deposition, in our case taken to be modern-day measurements from the far north of New Zealand ([Chen et al., 1985](#)). In contrast to P, elements that are relatively immobile and not biologically utilised, such as Pb, U, and Cu ([Novak et al., 2011](#); [Mikutta et al., 2016](#)), increased in absolute (numerical) terms at times of high CAR ([Supplementary Figure S3](#)) and, moreover, were positively correlated with CAR, increasing at the time of the eruptive events.

As noted earlier, volcanic eruptions add nutrients through atmospheric deposition, including contributing P ([Mahowald et al., 2008](#)), both directly through the deposition of compounds containing PO<sub>4</sub><sup>3-</sup> that are derived from volcanic aerosols, and indirectly through the addition of various acidic aerosols – which aid dissolution processes – and the P-bearing glass shards or pumice fragments, and apatite crystals. Glass is very rapidly dissolved via hydrolysis because it is thermodynamically unstable and, being fragmental and often vesicular and porous, has a high surface area to volume ratio and hence breaks down very quickly and at rates closely proportional to geometric surface areas ([Wolff-Boenisch et al., 2004](#); [Churchman and Lowe, 2012](#)).

High concentrations of P can occur within eruptive plumes (where it is rapidly oxidised including as PO<sub>4</sub><sup>3-</sup>), which is typically related to the P content of the parent magma ([Bergametti et al., 1984](#); [Mahowald et al., 2008](#); [Roberts et al., 2019](#)). Metal and crystalline salts, along with volcanic aerosol-derived acids, are adsorbed on volcanic particles as the eruption plume cools ([Óskarsson, 1980](#)), and high concentrations of phosphoric and other acid aerosols have been found adsorbed onto glass shards ([Frogner](#)

[et al., 2001](#); [Cronin et al., 2003](#)), which are then rapidly released upon contact with water. Therefore, either salts or phosphoric acid aerosols generated during an eruption would provide an almost instantaneous input of P into the ecosystem, along with hydronium ions that will enact the dissolution of accompanying glass and mineral particles deposited on the bog surface.

The indirect route for P to enter Moanatuatua Bog would have been through the rapid weathering (dissolution) of volcanic glass shards and apatite crystals, both in situ after deposition on the peat surface, or earlier within the eruptive plume. Within the eruptive plume, strong acids such as hydrofluoric acid can strip bases, such as phosphate, from the glass and apatite particles, sometimes to such an extent that the leachates can become effectively neutralised ([Dethier et al., 1981](#); [Herre et al., 2007](#)). Uranium, copper, and lead are primarily mobilised this way through the chemical 'enleaching' of glass and crystal particles within the eruption column ([Smith et al., 1982](#)).

Glass shards from the rhyolitic Ka and Tp tephra, and from the andesitic-dacitic Tf4, Tf5, and Tf6 cryptotephra, at Moanatuatua Bog contain small or trace amounts of P (reported as P<sub>2</sub>O<sub>5</sub>) ([Gehrels, 2009](#)) ([Table 3](#)). As described earlier, volcanic glass can dissolve very rapidly within the acidic bog conditions, releasing P ([Le Roux et al., 2006](#)). [Gehrels \(2009\)](#) reported heavy pitting of glass shards at Moanatuatua, particularly of the brown, andesitic to dacitic shards (Tf4, Tf5 & Tf6) which contain higher amounts of P than the colourless rhyolitic shards ([Table 3](#)).

Although volcanic glass (including pumiceous forms) is overwhelmingly predominant in the five tephra/cryptotephra in Moanatuatua discussed above, these tephra/cryptotephra deposits also contain the phosphate-group mineral, apatite, in small amounts. Both Tp and Ka contain essential or accessory amounts of apatite ([Ewart, 1963](#); [Lowe, 1988](#); [Nairn et al., 2004](#)). Further, natural spring waters fed from water passing through multiple Holocene Taupo-volcano-derived tephra are enriched in P ([Timperley, 1983](#)). [Cronin et al. \(2003\)](#) reported that fluorapatite was deposited during the 1995-96 eruptions of Mt Ruapehu, and the same mineral is likely to have accompanied deposition from the Mt Ruapehu-sourced Tufa Trig tephra identified in Moanatuatua Bog by [Gehrels \(2009\)](#). The weathering of apatite in volcanic soils is well documented with even the relatively weak carbonic acid produced from microbially respired CO<sub>2</sub> able to mobilise phosphorus from volcanically-derived apatite ([Nanzyo, 2002](#); [Dahlgren et al., 2004](#)). The stronger humic acids, which are abundant in peatlands, together with the aerosolic acids deposited concomitantly with glass and crystal particles during an eruption, can also facilitate the

dissolution of apatite, making it available for biological uptake (Lobartini et al., 1994); this can happen relatively quickly with the combined presence of apatite and humic acids able to boost plant growth in as little as 30 days (Lobartini et al., 1994). Naturally-occurring apatite was found to completely dissolve within 20 years of deposition in a German raised bog (Le Roux et al., 2006), and biotite was totally removed rapidly from the Kaharoa Tephra in Kopuatai bog (Hodder et al., 1991).

The mean accumulation rate of P in Moanatuatua of  $0.015 \text{ g m}^{-2} \text{ yr}^{-1}$  is remarkably similar to that of UK peatlands,  $0.017 \text{ g m}^{-2} \text{ yr}^{-1}$  (Schillereff et al., 2016), and for rates measured in peatlands in Ontario, Canada,  $0.016 \text{ g C m}^{-2} \text{ yr}^{-1}$  (Wang et al., 2015a). However, both the C:P (3448) and N:P (98) ratios are greater at Moanatuatua than most values in reported in the literature. For instance, a mean C:P of 1405 and C:N of 40 was found for a range of UK bogs (Schillereff et al., 2016), whereas a mean C:P of 2000:1 was found for 400 peat profiles in Canada (Wang et al., 2015a). Moorehouse bog in the UK is the exception to this with a C:P value at 30 cm depth of 4240 (Worrall et al., 2016). The C:P ratio is thought to be so low at Moorehouse because of the long history of sheep grazing at the site and associated phosphorus removal from the ecosystem (Worrall et al., 2016). At Moanatuatua the exceptionally low P concentration could be due to the presence of cluster roots in the dominant peat former, *E. robustum*, at Moanatuatua, which are known to be highly efficient at recovering P from organic matter via carboxylate extrudation (Lambers et al., 2012, 2013). In Canada, Wang et al., 2015a found a strong positive relationship ( $R^2 = 0.69$ ) between C and P accumulation rates, and a similarly strong relationship ( $R^2 = 0.76$ ) between C and N accumulation rates. Here we found even stronger relationships for CAR and P ( $R^2 = 0.90$ ), and for C and N accumulation rates ( $R^2 = 0.97$ ) (Fig. 9), suggesting greater control of CAR by nutrient inputs. This close relationship is perhaps to be expected given both the shorter time period investigated and the high variation in nutrient inputs attributed to the five tephra/cryptotephra depositional events. However, the relationship could also be a consequence of the weaker influence of climate on C accumulation in the highly oceanic, mild climate of the North Island of New Zealand. For example, metrics such as photosynthetically active radiation summed over the growing season, purported to be an important driver of long-term C dynamics in the Northern Hemisphere (Gallego-sala et al., 2018), are less meaningful for the present-day Moanatuatua where growth can occur year-round (Campbell et al., 2014) and photosynthesis can be light-saturated throughout most of the year (Goodrich et al., 2015).

During periods of rapid C accumulation, concentrations of elements taken up by plant growth, but not limiting to plant growth, such as Mg and Ca, become depleted (Fig. 7). Although we are more cautious in interpreting the variations in the abundance of these elements as they are soluble and move around within the profile, nevertheless changes in their concentration are consistent with rapid peat accumulation (Wang et al., 2015a).

Our study adds to a growing body of literature showing the importance of atmospheric inputs as a driver of C accumulation in ombrotrophic bogs (Glaser et al., 2013; Fiałkiewicz-Kozieł et al., 2016; Kylander et al., 2018). P deposition in the central North Island of New Zealand,  $0.040 \text{ g C m}^{-2} \text{ yr}^{-1}$  (Fish, 1976; Tipping et al., 2014), is above the global average, and higher than rates of  $0.015 \text{ g C m}^{-2} \text{ yr}^{-1}$  in the far north of New Zealand (Chen et al., 1985) and it should be noted that long term P accumulation at Moanatuatua ( $0.015 \text{ g C m}^{-2} \text{ yr}^{-1}$ ) matches P deposition rates for the far north. High fertiliser drift due to aerial topdressing has been found to alter the nutrient dynamics and successional ecology of New Zealand forests located less than 30 km from our study site (Stevenson, 2004). New Zealand is also experiencing elevated aeolian dust inputs because of land-use change in Australia (Brahney et al., 2019).

These local changes are part of a wider global trend of elevated P deposition (Brahney et al., 2015) with almost half of atmospherically-deposited P estimated to be derived from the burning of fossil fuel (Wang et al., 2015b), and a significant amount suspected to be from land-use change (Brahney et al., 2015). For example, remote, alpine ecosystems in the western United States have undergone more than a fivefold increase in inputs of K, Mg, Ca, N, and P since the start of the 19th century, which is attributed primarily to increased agricultural activity (Neff et al., 2008). Elsewhere, monitoring sites in Europe, located close to farmland, register rates of P input which are an order of magnitude higher than the global average (Tipping et al., 2014). In other instances, human activities have caused an increase in dust inputs into ecosystems (McConnell et al., 2007; Fiałkiewicz-Kozieł et al., 2016, 2020; Mullan-Boudreau et al., 2017), which implies greater atmospheric deposition of P. Considering the sensitivity of CAR at Moanatuatua Bog to periods of enhanced inorganic deposition from tephra (and associated aerosol) fallout, we suggest that the high rate of  $\text{CO}_2$  uptake in the present day (e.g.  $69 \text{ g C cm}^{-2} \text{ yr}^{-1}$  for Moanatuatua and  $203 \text{ g C cm}^{-2} \text{ yr}^{-1}$  for Kopuatai as reported in Ratcliffe et al., 2019) could be due to increased P inputs, potentially from local and distant sources, but this hypothesis would need to be verified through monitoring of present-day P deposition.

## 5. Conclusions

In the context of 21st-century changes to global nutrient cycling, it is important to understand how peatlands have responded to nutrient inputs in the past. We measured elemental accumulation across a c. 1000 year period in a northern New Zealand bog spanning two large volcanic depositional events and three smaller events. Volcanoes can deliver phosphorus to ecosystems through a variety of mechanisms, and the presence of the phosphate-rich mineral apatite and the presence of phosphorus within easily-weatherable volcanic glass support the contention that volcanic eruptions have been a source of elevated phosphorus inputs into Moanatuatua Bog.

We found peatland carbon accumulation rates to be highly coupled to nitrogen and phosphorus accumulation, with quite consistent stoichiometric ratios being maintained, allowing CAR to increase rapidly following ash deposition from eruptive events. All the same, deposition of volcanic material coincided with small shifts in stoichiometric ratios, indicating a greater abundance of phosphorus during these times. Such events coincided with increases in the concentration of trace metals of volcanic origin with a high affinity for organic matter such as lead, uranium, and copper, providing evidence for acidic leaching of elements from volcanic glass, either within the eruption plume or following deposition in the peatland, or both.

We conclude that long-term carbon accumulation rates in New Zealand bogs were, and likely still are, primarily constrained by nutrients rather than direct climatic drivers such as temperature or moisture availability. Similar findings, pointing to the pivotal role of phosphorus in peatland C cycling in Japanese (Hughes et al., 2013) and Swedish bogs (Kylander et al., 2018), suggests this phenomenon could be widespread. It is notable that, despite a large number of investigations, peatland long-term carbon accumulation has only been found to have a relatively weak correlation with climatic variables (e.g. the strongest climatic correlation found by Gallego-sala et al., 2018 was an  $R^2$  of 0.2 for photosynthetically active radiation summed over the growing season). This observation is in stark contrast with the results presented here, and in a small number of other studies, which have also considered past nutrient inputs. Our results, and those of the aforementioned studies, show that nutrients, phosphorus in particular, exert a strong influence on

long-term peatland carbon dynamics. Phosphorus inputs, at least in some peatlands, may exert a greater influence on peatland carbon accumulation than direct climatic forcing.

## Dedication

This paper is dedicated to the memory of Dr Richard J. Payne (1978–2019). Richard conducted his science in a highly amicable way with a strong emphasis on collaboration and shared successes. Richard, who guided Ratcliffe firstly in his masterate and then in subsequent research, continued to provide great encouragement and generous, selfless advice up until his untimely death (see Bunting et al., 2020 and Mazei et al., 2020).

## Declaration of competing interest

The authors declare that they have no known competing financial interests or personal relationships that could have appeared to influence the work reported in this paper.

## Acknowledgements

We thank Bev Clarkson, Bruce Clarkson, Tim Moore, Mahdiyeh Salmanzadeh and (the late) Richard Payne, for informative discussions on the topics in this paper. We also thank Scott Bartlam for assistance in the field, and Noel Bates, Judith Houl, and Annie Barker for their assistance in the lab. Rewi Newnham and Ignacio Jara offered helpful advice on choosing the coring location, while Greg Furniss from Blueberry Country kindly facilitated access to the coring site and his blueberry orchard. Prof Newnham's supervisory role in the earlier research undertaken by Gehrels (2009), a component of which is reported here, is also acknowledged. Our research was supported by SSIF funding for Crown Research Institutes from the Ministry of Business, Innovation and Employment's Science and Innovation Group via Manaaki Whenua Landcare Research. The authors would also like to acknowledge the Department of Conservation staff for their work administering the reserve and the Ngā Iwi Tōpū O Waipā, who represent the traditional kaitiaki of Moanatuatua. We would also like to thank two anonymous reviewers for their very constructive input and suggestions.

## Appendix A. Supplementary data

Supplementary data to this article can be found online at <https://doi.org/10.1016/j.quascirev.2020.106505>.

## References

Abella, S.E.B., 1988. The effect of the Mt. Mazama ashfall on the planktonic diatom community of Lake Washington. *Limnol. Oceanogr.* 33, 1376–1385.

Aerts, R., Wallen, B., Malmer, N., 1992. Growth-limiting nutrients in sphagnum-dominated bogs subject to low and high atmospheric nitrogen supply. *J. Ecol.* 80, 131. <https://doi.org/10.2307/2261070>.

Allen, L.R., 1948. Activity at Ngauruhoe, april–may 1948. *N. Z. J. Sci. Technol.* 30, 187–193.

Belokopytov, I.E., Beresnevich, V.V., 1955. Giktorf's peat borers (in Russian). *Torfanaa Promislenost* 8, 9–10.

Bergametti, G., Martin, D., Carbone, J., Favier-Pierret, R., Le Sage, R.V., 1984. A mesoscale study of the elemental composition of aerosols emitted from Mt. Etna Volcano. *Bull. Volcanol.* 47, 1107–1114. <https://doi.org/10.1007/BF01952366>.

Blaauw, M., Christen, A., 2011. Flexible paleoclimate age-depth models using an autoregressive gamma process. *Bayesian Anal.* 6, 457–474. <https://doi.org/10.1214/11-BA618>.

Blockley, S.P.E., Pyne-O'Donnell, S.D.F., Lowe, J.J., Matthews, I.P., Stone, A., Pollard, A.M., Turney, C.S.M., Molyneux, E.G., 2005. A new and less destructive laboratory procedure for the physical separation of distal glass tephra shards from sediments. *Quat. Sci. Rev.* 24, 1952–1966.

Bragazza, L., Buttler, A., Habermacher, J., Brancaloni, L., Gerdol, R., Fritze, H.,

Hanajik, P., Laiho, R., Johnson, D., 2012. High nitrogen deposition alters the decomposition of bog plant litter and reduces carbon accumulation. *Global Change Biol.* 18, 1163–1172. <https://doi.org/10.1111/j.1365-2486.2011.02585.x>.

Brahney, J., Ballantyne, A.P., Vandergoes, M., Baisden, T., Neff, J.C., 2019. Increased dust deposition in New Zealand related to twentieth century Australian land use. *J. Geophys. Res. Biogeosci.* 1181–1193. <https://doi.org/10.1029/2018JG004627>.

Brahney, J., Mahowald, N., Ward, D.S., Ballantyne, A.P., Neff, J.C., 2015. Is atmospheric phosphorus pollution altering global alpine lake stoichiometry? *Global Biogeochem. Cycles* 29. <https://doi.org/10.1002/2015GB005137>. Received, 1369–1363.

Bunting, M.J., Blackford, J., Gehrels, M.J., Gehrels, W.R., 2020. In memoriam and dedication: richard john payne (1978–2019). *J. Quat. Sci.* 35, 9–10.

Campbell, D.I., Smith, J., Goodrich, J.P., Wall, A.M., Schipper, L.A., 2014. Year-round growing conditions explains large CO<sub>2</sub> sink strength in a New Zealand raised peat bog. *Agric. For. Meteorol.* 192–193, 59–68. <https://doi.org/10.1016/j.jagromet.2014.03.003>.

Chambers, F.M., Beilman, D.W., Yu, Z., 2011. Methods for determining peat humification and for quantifying peat bulk density, organic matter and carbon content for palaeostudies of climate and peatland carbon dynamics. *Mires Peat* 7, 1–10.

Chen, L., Arimoto, R., Duce, R.A., 1985. The sources and forms of phosphorus in marine aerosol particles and rain from Northern New Zealand. *Atmos. Environ.* 19, 779–787. [https://doi.org/10.1016/0004-6981\(85\)90066-6](https://doi.org/10.1016/0004-6981(85)90066-6).

Churchman, G.J., Lowe, D.J., 2012. Alteration, formation, and occurrence of minerals in soils. In: *Handbook of Soil Sciences*, second ed., vol. 1. Properties and Processes. CRC Press (Taylor & Francis), Boca Raton, Florida, USA, pp. 20.1–20.72.

Clarkson, B.R., 1997. Vegetation recovery following fire in two Waikato peatlands at Whangamarino and Moanatuatua, New Zealand. *N. Z. J. Bot.* 35, 167–179. <https://doi.org/10.1080/0028825X.1997.10414153>.

Clarkson, B.R., Schipper, L.A., Moyersoen, B., Silvester, W.B., 2005. Foliar 15N natural abundance indicates phosphorus limitation of bog species. *Oecologia* 144, 550–557. <https://doi.org/10.1007/s00442-005-0033-4>.

Clarkson, B.R., Schipper, L.A., Silvester, W.B., 2009. Nutritional niche separation in coexisting bog species demonstrated by 15N-enriched simulated rainfall. *Austral Ecol.* 34, 377–385. <https://doi.org/10.1111/j.1442-9993.2009.01939.x>.

Clarkson, B.R., Cave, V.M., Watts, C.H., Thornburrow, D., Fitzgerald, N.B., 2020. Effects of lowered water table and agricultural practices on a remnant restiad bog over four decades. *Mires Peat* 26, 1–13.

Cranwell, L.M., 1939. Native vegetation. In: *Soils and Agriculture of Part of Waipā County*. Dept. Of Scientific and Industrial Research. Bulletin, vol. 76, pp. 23–29. <https://doi.org/10.7931/DL1-SBP-0005>.

Cronin, S.J., Neall, V.E., Lecoindre, J.A., Hedley, M.J., Loganathan, P., 2003. Environmental hazards of fluoride in volcanic ash: a case study from Ruapehu volcano, New Zealand. *J. Volcanol. Geoth. Res.* 121, 271–291. [https://doi.org/10.1016/S0377-0273\(02\)00465-1](https://doi.org/10.1016/S0377-0273(02)00465-1).

Dahlgren, R.A., Saigusa, M., Ugolini, F.C., 2004. The nature, properties and management of volcanic soils. *Adv. Agron.* 82, 113–182.

Damman, A.W.H., 1986. Hydrology, development, and biogeochemistry of ombrogenous peat bogs with special reference to nutrient relocation in a western Newfoundland bog. *Can. J. Bot.* 64, 384–394. <https://doi.org/10.1139/b86-055>.

Dargie, G.C., Lewis, S.L., Lawson, I.T., Mitchard, E.T.A., Page, S.E., Bocko, Y.E., Ifo, S.A., 2017. Age, extent and carbon storage of the central Congo Basin peatland complex. *Nature* 542, 86–90. <https://doi.org/10.1038/nature21048>.

Davoren, A., 1978. A Survey of New Zealand Peat Resources, vol. 14. Ministry of Works, Water and Soil Technical Publication, p. 157. + maps).

de Lange, P.J., Lowe, D.J., 1990. History of vertical displacement of kerepehi fault at kopouatai bog, hauraki lowlands, New Zealand, since c. 10 700 years ago. *N. Z. J. Geol. Geophys.* 33, 277–283. <https://doi.org/10.1080/00288306.1990.10425685>.

de Lange, P.J., Heenan, P.B., Clarkson, B.D., Clarkson, B.R., 1999. Taxonomy, ecology, and conservation of sporodanthus (restionaceae) in New Zealand. *N. Z. J. Bot.* 37, 413–431.

Delmelle, P., Maters, E., Oppenheimer, C., 2015. Volcanic influences on the carbon, sulfur, and halogen biogeochemical cycles. *The Encyclopedia of Volcanoes*. Elsevier, pp. 881–893.

Dethier, D.P., Pevear, D.R., Frank, D., 1981. Alteration of new volcanic deposits. In: Lipman, P.W., Mullineaux, D.R. (Eds.), *The 1980 Eruptions of Mount St. Helens, Washington*. Geological Survey Professional Paper 1250. United States Government Printing Office, Washington, DC, pp. 649–665.

Donoghue, S.L., Neall, V.E., Palmer, A.S., Stewart, R.B., 1997. The volcanic history of Ruapehu during the past 2 millennia based on the record of Tufa Trig tephra. *Bull. Volcanol.* 59, 136–146. <https://doi.org/10.1007/s004450050181>.

Einarsson, A., Óskarsson, H., Hafliðason, H., 1993. Stratigraphy of fossil pigments and Cladophora and its relationship with deposition of tephra in Lake Mývatn, Iceland. *J. Paleolimnol.* 8, 15–26.

Ewart, A., 1963. Petrology and petrogenesis of the Quaternary pumice ash in the Taupo area, New Zealand. *J. Petrol.* 4, 392–431.

Fialkiewicz-Kozieł, B., Smieja-Król, B., Frontasyeva, M., Stowiński, M., Marcisz, K., Lapszina, E., Gilbert, D., Buttler, A., Jassey, V.E.J., Kalisz, K., Laggoun-Défarge, F., Kolaček, P., Lamentowicz, M., 2016. Anthropogenic- and natural sources of dust in peatland during the Anthropocene. *Sci. Rep.* 6, 1–8. <https://doi.org/10.1038/srep38731>.

Fialkiewicz-Kozieł, B., Łokas, E., Gałka, M., Kolaček, P., De Vleeschouwer, F., Le Roux, G., Smieja-Król, B., 2020. Influence of transboundary transport of trace

- elements on mountain peat geochemistry (Sudetes, Central Europe). *Quat. Sci. Rev.* 230, 106162. <https://doi.org/10.1016/j.quascirev.2020.106162>.
- Fish, G.R., 1976. The fallout of nitrogen and phosphorus compounds from the atmosphere at ngapuna, near rotorua, New Zealand. *N. Z. J. Hydrol.* 15, 27–34.
- Frogner, P., Gíslason, S.R., Óskarsson, N., 2001. Fertilizing potential of volcanic ash in ocean surface water. *Geology* 29, 487–490. [https://doi.org/10.1130/0091-7613\(2001\)029<0487:FPOVAI>2.0.CO;2](https://doi.org/10.1130/0091-7613(2001)029<0487:FPOVAI>2.0.CO;2).
- Gallego-sala, A.V., Charman, D.J., Brewer, S., Page, S.E., Prentice, I.C., Friedlingstein, P., Moreton, S., Amesbury, M.J., Beilman, D.W., Björck, S., Blyakharchuk, T., Bochicchio, C., Booth, R.K., Bunbury, J., Carless, D., Chimner, R.A., Clifford, M., Cressey, E., Finkelstein, S.A., Gorneau, M., Githumbi, E., Hribljan, J., Holmquist, J., Nichols, J., Oksanen, P.O., Orme, L., Packalen, M.S., Robinson, S., Swindles, G.T., Turner, T.E., Uglow, J., Väliiranta, M., 2018. Latitudinal limits to the predicted increase of the peatland carbon sink with warming. *Nat. Clim. Change* 8, 907–913.
- Gehrels, M.J., 2009. An Enhanced ~1800-Year Record of Recent Volcanic Ash-Fall Events for Northern New Zealand from the Analysis of Cryptotephra. Unpublished PhD thesis, University of Plymouth, UK.
- Gehrels, M.J., Lowe, D.J., Hazell, Z.J., Newnham, R.M., 2006. A continuous 5300-yr Holocene cryptotephrostratigraphic record from northern New Zealand and implications for tephrochronology and volcanic-hazard assessment. *Holocene* 16, 173–187.
- Gehrels, M.J., Lowe, D.J., Newnham, R.M., Hogg, A.G., 2010. Enhanced record of tephra fallout since ~232 AD revealed by cryptotephra studies at Moanatuatua Bog near Hamilton: implications for volcanic hazard analysis. *Geosci. Soc. New Zeal. Misc. Publ. A* 129, 103.
- Giles, T.M., 1999. Volcanic Emissions and Distal Palaeoenvironmental Impacts in New Zealand. Unpublished PhD thesis, University of Plymouth, UK.
- Glaser, P.H., Hansen, B.C.S., Donovan, J.J., Givnish, T.J., Stricker, C.A., Volin, J.C., 2013. Holocene dynamics of the Florida Everglades with respect to climate, dustfall, and tropical storms. *Proc. Natl. Acad. Sci. Unit. States Am.* 110, 17211–17216. <https://doi.org/10.1073/pnas.1222239110>.
- Gogo, S., Laggoun-Défarge, F., Delarue, F., Lottier, N., 2011. Invasion of a Sphagnum-peatland by *Betula* spp and *Molinia caerulea* impacts organic matter biochemistry. Implications for carbon and nutrient cycling. *Biogeochemistry* 106, 53–69. <https://doi.org/10.1007/s10533-010-9433-6>.
- Goodrich, J.P., Campbell, D.I., Clearwater, M.J., Rutledge, S., Schipper, L.A., 2015. High vapor pressure deficit constrains GPP and the light response of NEE at a Southern Hemisphere bog. *Ag Met* 203, 54–63. <https://doi.org/10.1016/j.agrformet.2015.01.001>.
- Goodrich, J.P., Campbell, D.I., Schipper, L.A., 2017. Southern Hemisphere bog persists as a strong carbon sink during droughts. *Biogeosciences* 14, 4563–4576. <https://doi.org/10.5194/bg-14-4563-2017>.
- Goring, S., Williams, J.W., Blois, J.L., Jackson, S.T., Paciorek, C.J., Booth, R.K., Marlon, J.R., Blaauw, M., Christen, J.A., 2012. Deposition times in the north-eastern United States during the Holocene: establishing valid priors for Bayesian age models. *Quat. Sci. Rev.* 48, 54–60. <https://doi.org/10.1016/j.quascirev.2012.05.019>.
- Green, J.D., Lowe, D.J., 1985. Stratigraphy and development of c. 17 000 year old Lake Maratoto, North Island, New Zealand, with some inferences about postglacial climatic change. *N. Z. J. Geol. Geophys.* 28, 675–699. <https://doi.org/10.1080/00288306.1985.10422541>.
- Gunnarsson, T.G., Arnalds, O., Appleton, G., Méndez, V., Gill, J.A., 2015. Ecosystem recharge by volcanic dust drives broad-scale variation in bird abundance. *Ecol. Evol.* 5, 2386–2396.
- Haenfling, C., Newnham, R., Rees, A., Jara, I., Homes, A., Clark, B., 2017. Holocene history of a raised bog, northern New Zealand, based on plant cuticles. *Holocene* 27, 309–314. <https://doi.org/10.1177/0959683616658524>.
- Harper, M.A., Howorth, R., McLeod, M., 1986. Late Holocene diatoms in Lake Poukawa: effects of airfall tephra and changes in depth. *N. Z. J. Mar. Freshw. Res.* 20, 107–118. <https://doi.org/10.1080/00288330.1986.9516135>.
- Herre, A., Lang, F., Siebe, C.H., Dorhmann, R., Kaupenjohann, M., 2007. Mechanisms of acid buffering and formation of secondary minerals in vitric Andosols. *Eur. J. Soil Sci.* 58, 431–444. <https://doi.org/10.1111/j.1365-2389.2007.00890.x>.
- Hodder, A.P.W., de Lange, P.J., Lowe, D.J., 1991. Dissolution and depletion of ferromagnesian minerals from Holocene tephra later in an acid bog, New Zealand, and implications for tephra correlation. *J. Quat. Sci.* 6, 195–208.
- Hogg, A., Lowe, D.J., Palmer, J., Boswijk, G., Bronk Ramsey, C., 2012. Revised calendar date for the Taupo eruption derived by 14C wiggle-matching using a New Zealand kauri 14C calibration data set. *Holocene* 22, 439–449. <https://doi.org/10.1177/0959683611425551>.
- Hogg, A.G., Higham, T.F.G., Lowe, D.J., Palmer, J.G., Reimer, P.J., Newnham, R.M., 2003. A wiggle-match date for Polynesian settlement of New Zealand. *Antiquity* 77, 116–125. <https://doi.org/10.1017/S0003598X00061408>.
- Hogg, A.G., Hua, Q., Blackwell, P.G., Niu, M., Buck, C.E., Guilderson, T.P., Zimmerman, S.R.H., 2013. SHCal13 Southern Hemisphere calibration, 0–50,000 years cal BP. *Radiocarbon* 55, 1–15. [https://doi.org/10.2458/azu\\_js\\_rc.55.16783](https://doi.org/10.2458/azu_js_rc.55.16783).
- Hogg, A.G., Wilson, C.J.N., Lowe, D.J., Turney, C.S.M., White, P., Lorrey, A.M., Manning, S.W., Palmer, J.G., Bury, S., Brown, J., Southon, J., Petchey, F., 2019. Wiggle-match radiocarbon dating of the Taupo eruption. *Nat. Commun.* 10, 4669. <https://doi.org/10.1038/s41467-019-12532-8>.
- Hotes, S., Poschod, P., Takahashi, H., 2006. Effects of volcanic activity on mire development: case studies from Hokkaido, northern Japan. *Holocene* 16, 561–573. <https://doi.org/10.1191/0959683606h1952rp>.
- Hunt, J.B., Hill, P.G., 1993. Tephra geochemistry: a discussion of some persistent analytical problems. *Holocene* 3, 271–278.
- Hughes, P.D.M., Mallon, G., Brown, a., Essex, H.J., Stanford, J.D., Hotes, S., 2013. The impact of high tephra loading on late-Holocene carbon accumulation and vegetation succession in peatland communities. *Quat. Sci. Rev.* 67, 160–175. <https://doi.org/10.1016/j.quascirev.2013.01.015>.
- Hutchinson, S.J., Hamilton, P.B., Patterson, R.T., Galloway, J.M., Nasser, N.A., Spence, C., Falk, H., 2019. Diatom ecological response to deposition of the 833–850 CE White River Ash (east lobe) ashfall in a small subarctic Canadian lake. *PeerJ* 7, e6269. <https://doi.org/10.7717/peerj.6269>.
- Jara, I.A., Newnham, R.M., Alloway, B.V., Wilmshurst, J.M., Rees, A.B., 2017. Pollen-based Temperature and Precipitation Records of the Past 14,600 Years in Northern New Zealand (37°S) and Their Linkages with the Southern Hemisphere Atmospheric Circulation. *The Holocene* 095968361770844. <https://doi.org/10.1177/0959683617708444>.
- Jowsey, P.C., 1966. An improved peat sampler. *New Phytol.* 65, 245–248. <https://doi.org/10.1111/j.1469-8137.1966.tb06356.x>.
- Kylander, M.E., Rauch, S., Hansson, S.V., Rydberg, J., Kaal, J., Mörtz, C.-M., Silva-Sánchez, N., Gallagher, K., Greenwood, S.L., Bindler, R., Martínez-Cortizas, A., Sjöström, J.K., 2018. Mineral dust as a driver of carbon accumulation in northern latitudes. *Sci. Rep.* 8, 1–10. <https://doi.org/10.1038/s41598-018-25162-9>.
- Lambers, H., Bishop, J.G., Hopper, S.D., Laliberté, E., Zúñiga-Feest, A., 2012. Phosphorus-mobilization ecosystem engineering: the roles of cluster roots and carboxylate exudation in young P-limited ecosystems. *Ann. Bot.* 110, 329–348. <https://doi.org/10.1093/aob/mcs130>.
- Lambers, H., Clements, J.C., Nelson, M.N., 2013. How a phosphorus-acquisition strategy based on carboxylate exudation powers the success and agronomic potential of lupines (*Lupinus*, Fabaceae). *Am. J. Bot.* 100, 263–288. <https://doi.org/10.3732/ajb.1200474>.
- Le Quéré, C., Andrew, R.M., Friedlingstein, P., Sitch, S., Hauck, J., Pongratz, J., Pickers, P., Korsbakken, J.I., Peters, G.P., Canadell, J.G., others, 2018. Global carbon budget 2018. *Earth Syst. Sci. Data* 10, 2141–2194.
- Le Roux, G., Laverret, E., Shoty, W., 2006. Fate of calcite, apatite and feldspars in an ombrotrophic peat bog, Black Forest, Germany. *J. Geol. Soc. Londn.* 163, 641–646. <https://doi.org/10.1144/0016-764920-035>.
- Limpens, J., Berendse, F., Klees, H., 2003. N deposition affects N availability in interstitial water, growth of Sphagnum and invasion of vascular plants in bog vegetation. *New Phytol.* 157, 339–347. <https://doi.org/10.1046/j.1469-8137.2003.00667.x>.
- Liu, L., Chen, H., Liu, X., Yang, Z., Zhu, D., He, Y., Liu, J., 2019. Contemporary, modern and ancient carbon fluxes in the Zoige peatlands on the Qinghai-Tibetan Plateau. *Geoderma* 352, 138–149. <https://doi.org/10.1016/j.geoderma.2019.06.008>.
- Lobartini, J.C., Tan, K.H., Pape, C., 1994. The nature of humic acid-apatite interaction products and their availability to plant growth. *Commun. Soil Sci. Plant Anal.* 25, 2355–2369. <https://doi.org/10.1080/00103629409369193>.
- Lowe, D.J., 1988. Stratigraphy, age, composition, and correlation of late Quaternary tephras interbedded with organic sediments in Waikato lakes, North Island, New Zealand. *N. Z. J. Geol. Geophys.* 31, 125–165. <https://doi.org/10.1080/00288306.1988.10417765>.
- Lowe, D.J., 2011. Tephrochronology and its application: a review. *Quat. Geochronol.* 6, 107–151. <https://doi.org/10.1016/j.quageo.2010.08.003>.
- Lowe, D.J., Pearce, N.J.G., Jorgensen, M.A., Kuehn, S.C., Tryon, C.A., Hayward, C.L., 2017. Correlating tephras and cryptotephras using glass compositional analyses and numerical and statistical methods: review and evaluation. *Quat. Sci. Rev.* 175, 1–44. <https://doi.org/10.1016/j.quascirev.2017.08.003>.
- Lu, W., Xiao, J., Liu, F., Zhang, Y., Liu, C., Lin, G., 2017. Contrasting ecosystem CO<sub>2</sub> fluxes of inland and coastal wetlands: a meta-analysis of eddy covariance data. *Global Change Biol.* 23, 1180–1198. <https://doi.org/10.1111/gcb.13424>.
- Lund, M., Christensen, T.R., Mastepanov, M., Lindroth, A., Ström, L., 2009. Effects of N and P fertilization on the greenhouse gas exchange in two northern peatlands with contrasting N deposition rates. *Biogeosciences* 6, 2135–2144. <https://doi.org/10.5194/bg-6-2135-2009>.
- Mahowald, N., Jickells, T.D., Baker, A.R., Artaxo, P., Benitez-Nelson, C.R., Bergametti, G., Bond, T.C., Chen, Y., Cohen, D.D., Herut, B., Kubilay, N., Losno, R., Luo, C., Maenhaut, W., McGee, K.A., Okin, G.S., Siefert, R.L., Tsukuda, S., 2008. Global distribution of atmospheric phosphorus sources, concentrations and deposition rates, and anthropogenic impacts. *Global Biogeochem. Cycles* 22, 1–19. <https://doi.org/10.1029/2008GB003240>.
- Marx, S.K., McGowan, H.A., Kamber, B.S., 2009. Long-range dust transport from eastern Australia: a proxy for Holocene aridity and ENSO-type climate variability. *Earth Planet Sci. Lett.* 282, 167–177.
- Matheson, K.S., 1979. Moanatuatua – an Ecological Study of an Oligotrophic, Restiad Bog, Waikato, New Zealand. Unpublished MSc thesis, University of Waikato, Hamilton, New Zealand.
- Mauquoy, D., Hughes, P., Geel, B. Van, 2010. A protocol for plant macrofossil analysis of peat deposits. *Mires Peat* 7, 1–5.
- Mazei, Y.A., Sapelko, T.V., Tsyganov, A.N., Novenko, E.Y., Lapshina, E.D., Zenkova, I.V., Babeshko, K.V., Esaulov, A.S., Kuprianov, D.A., Zarov, E.A., Tiunov, A.V., Mazei, N.G., Ratcliffe, J.L., Mauquoy, D., Sloan, T.J., Lamentowicz, M., Qin, Y., 2020. British ecologist and protistologist in Russia: in memoriam Dr. Richard John Payne (1978–2019) (in Russian). *Stud. Hist. Biol.* 12, 114–126. <https://doi.org/10.24411/2076-8176-2020-11006>.
- McConnell, J.R., Aristarain, A.J., Banta, J.R., Edwards, P.R., Simoes, J.C., 2007. 20th-century doubling in dust archived in an Antarctic Peninsula ice core parallels climate change and desertification in South America. *Proc. Natl. Acad. Sci. Unit.*

- States Am. 104, 5743–5748. <https://doi.org/10.1073/pnas.0607657104>.
- McGlone, M.S., Neall, V.E., Clarkson, B.D., 1988. The effect of recent volcanic events and climatic changes on the vegetation of Mt Egmont (Mt Taranaki), New Zealand. *N. Z. J. Bot.* 26, 123–144. <https://doi.org/10.1080/0028825X.1988.10410105>.
- McGlone, M.S., Neall, V.E., 1994. The late pleistocene and Holocene vegetation history of Taranaki, North Island, New Zealand. *N. Z. J. Bot.* 32, 251–269. <https://doi.org/10.1080/0028825X.1994.10410470>.
- Mullan-Boudreau, G., Davies, L., Devito, K., Froese, D., Noernberg, T., Pelletier, R., Shoty, W., 2017. Reconstructing past rates of atmospheric dust deposition in the Athabasca bituminous sands region using peat cores from bogs. *Land Degrad. Dev.* 28, 2468–2481.
- Mikutta, C., Langner, P., Bargar, J.R., Kretzschmar, R., 2016. Tetra- and hexavalent uranium forms bidentate-monoanuclear complexes with particulate organic matter in a naturally uranium-enriched peatland. *Environ. Sci. Technol.* 50, 10465–10475. <https://doi.org/10.1021/acs.est.6b03688>.
- Nairn, I.A., Shane, P.R., Cole, J.W., Leonard, G.J., Self, S., Pearson, N., 2004. Rhyolite magma processes of the AD 1315 Kaharoa eruption episode, Tarawera volcano, New Zealand. *J. Volcanol. Geoth. Res.* 131, 265–294.
- Nanzyo, M., 2002. Unique properties of volcanic-ash soils. *Global Environ. Res.* 6, 99–112.
- Neff, J.C., Ballantyne, A.P., Farmer, G.L., Mahowald, N.M., Conroy, J.L., Landry, C.C., Overpeck, J.T., Painter, T.H., Lawrence, C.R., Reynolds, R.L., 2008. Increasing eolian dust deposition in the western United States linked to human activity. *Nat. Geosci.* 1, 189–195. <https://doi.org/10.1038/ngeo133>.
- Nelson, C.S., 1975. Ngauruhoe ash fall in the Waikato. *Geol. Soc. N.Z. Newslett.* 39, 41–42.
- Newnham, R.M., Lowe, D.J., Gehrels, M.J., Augustinus, P., 2018. Two-step human–environmental impact history for northern New Zealand linked to late-Holocene climate change. *Holocene* 28, 1093–1106. <https://doi.org/10.1177/0959683618761545>.
- Newnham, R.M., Hazell, Z.J., Charman, D.J., Lowe, D.J., Rees, A.B.H., Amesbury, M.J., Roland, T.P., Gehrels, M., van den Bos, V., Jara, I.A., 2019. Peat humification records from Restionaceae bogs in northern New Zealand as potential indicators of Holocene precipitation, seasonality, and ENSO. *Quat. Sci. Rev.* 218, 378–394. <https://doi.org/10.1016/j.quascirev.2019.06.036>.
- Novak, M., Zemanova, L., Voldrichova, P., Stepanova, M., Adamova, M., Pacherova, P., Komarek, A., Krachler, M., Prechova, E., 2011. Experimental evidence for mobility/immobility of metals in peat. *Environ. Sci. Technol.* 45, 7180–7187. <https://doi.org/10.1021/es201086v>.
- Óskarsson, N., 1980. The interaction between volcanic gases and tephra: fluorine adhering to tephra of the 1970 hekla eruption. *J. Volcanol. Geoth. Res.* 8, 251–266. [https://doi.org/10.1016/0377-0273\(80\)90107-9](https://doi.org/10.1016/0377-0273(80)90107-9).
- Payne, R., Blackford, J., 2008. Distal volcanic impacts on peatlands: palaeoecological evidence from Alaska. *Quat. Sci. Rev.* 27, 2012–2030. <https://doi.org/10.1016/j.quascirev.2008.08.002>.
- Payne, R., Blackford, J., 2005. Simulating the impacts of distal volcanic products upon peatlands in northern Britain: an experimental study on the Moss of Achnacree, Scotland. *J. Archaeol. Sci.* 32, 989–1001. <https://doi.org/10.1016/j.jas.2005.02.001>.
- Payne, R.J., Ratcliffe, J.L., Andersen, R., Flitcroft, C.E., 2016. A meta-database of peatland palaeoecology in Great Britain. *Palaeogeogr. Palaeoclimatol. Palaeoecol.* 457, 389–395. <https://doi.org/10.1016/j.palaeo.2016.05.025>.
- Pearce, N.J.G., Abbott, P.M., Martin-Jones, C.M., 2014. Microbeam methods for the analysis of glass in fine grained tephra deposits: a SMART perspective on current and future trends. *Geol. Soc. Lond. Spec. Publ.* 398, 29–46.
- Pyne-O'Donnell, S.D.F., 2011. The taphonomy of Last Glacial–Interglacial Transition (LGIT) distal volcanic ash in small Scottish lakes. *Boreas* 131–145. <https://doi.org/10.1111/j.1502-3885.2010.00154.x>.
- Ratcliffe, J.L., Andersen, R., Anderson, R., Newton, A., Campbell, D., Mauquoy, D., Payne, R., 2018. Contemporary carbon fluxes do not reflect the long-term carbon balance for an Atlantic blanket bog. *Holocene* 28, 140–149. <https://doi.org/10.1177/0959683617715689>.
- Ratcliffe, J.L., Campbell, D.I., Clarkson, B.R., Schipper, L.A., Campbell, I.D., Clarkson, B.R., Schipper, L.A., 2019a. Water table fluctuations control CO<sub>2</sub> exchange in wet and dry bogs through different mechanisms. *Sci. Total Environ.* 655, 1037–1046. <https://doi.org/10.1016/j.scitotenv.2018.11.151>.
- Ratcliffe, J.L., Campbell, D.I., Schipper, L.A., Wall, A.M., Clarkson, B.R., 2020. Recovery of the CO<sub>2</sub> sink in a remnant peatland following water table lowering. *Sci. Total Environ.* 718 (134613) <https://doi.org/10.1016/j.scitotenv.2019.134613>.
- Reynolds, R., 1917. Development of peat swamps. *N. Z. J. Agric.* 15, 9–10.
- Roberts, T., Dayma, G., Oppenheimer, C., 2019. Reaction rates control high-temperature chemistry of volcanic gases in air. *Front. Earth Sci.* 7, 154. <https://doi.org/10.3389/feart.2019.00154>.
- Roland, T.P., Mackay, H., Hughes, P.D.M., 2015. Tephra analysis in ombrotrophic peatlands: a geochemical comparison of acid digestion and density separation techniques. *J. Quat. Sci.* 30, 3–8. <https://doi.org/10.1002/jqs.2754>.
- Schillereff, D.N., Boyle, J.F., Toberman, H., Adams, J.L., Bryant, C.L., Chivverrell, R.C., Helliwell, R.C., Keenan, P., Lilly, A., Tipping, E., 2016. Long-term macronutrient stoichiometry of UK ombrotrophic peatlands. *Sci. Total Environ.* 572, 1561–1572. <https://doi.org/10.1016/j.scitotenv.2016.03.180>.
- Shearer, J.C., 1997. Natural and anthropogenic influences on peat development in Waikato/Hauraki Plains restiad bogs. *J. Roy. Soc. N. Z.* 27, 295–313. <https://doi.org/10.1080/03014223.1997.9517540>.
- Sheppard, L.J., Leith, I.D., Mizunuma, T., Neil Cape, J., Crossley, A., Leeson, S., Sutton, M.A., Dijk, N., Fowler, D., 2011. Dry deposition of ammonia gas drives species change faster than wet deposition of ammonium ions: evidence from a long-term field manipulation. *Global Change Biol.* 17, 3589–3607. <https://doi.org/10.1111/j.1365-2486.2011.02478.x>.
- Smith, D.B., Zielinski, R.A., Rose, W.L., 1982. Leachability of uranium and other elements from freshly erupted volcanic ash. *J. Volcanol. Geoth. Res.* 13, 1–30. [https://doi.org/10.1016/0377-0273\(82\)90017-8](https://doi.org/10.1016/0377-0273(82)90017-8).
- Stevens, C.J., Lind, E.M., Hautier, Y., Harpole, W.S., Borer, E.T., Hobbie, S., Seabloom, E.W., Ladwig, L., Bakker, J.D., Chu, C., Collins, S., Davies, K.F., Firn, J., Hillebrand, H., La Pierre, K.J., MacDougall, A., Melbourne, B., McCulley, R.L., Morgan, J., Orrock, J.L., Prober, S.M., Risch, A.C., Schuetz, M., Wragg, P.D., Lind, E.M., Stevens, C.J., Seabloom, E.W., Hobbie, S., Morgan, J., Hillebrand, H., Harpole, W.S., Hautier, Y., Bakker, J.D., Firn, J., Chu, C., Melbourne, B., Risch, A.C., MacDougall, A., Pierre, K.J., La Pierre, S.M., Orrock, J.L., Ladwig, L., Collins, S., Schuetz, M., McCulley, R.L., Borer, E.T., Wragg, P.D., 2015. Anthropogenic nitrogen deposition predicts local grassland primary production worldwide. *Ecology* 96, 1459–1465. <https://doi.org/10.1890/14-1902.1>.
- Stevenson, B.A., 2004. Changes in phosphorus availability and nutrient status of indigenous forest fragments in pastoral New Zealand hill country. *Plant Soil* 262, 317–325.
- Stewart, C., Damby, D.E., Tomašek, I., Horwell, C.J., Plumlee, G.S., Armienta, M.A., Hinojosa, M.G.R., Appleby, M., Delmelle, P., Cronin, S., others, 2020. Assessment of leachable elements in volcanic ashfall: a review and evaluation of a standardized protocol for ash hazard characterization. *J. Volcanol. Geoth. Res.* 392.
- Timperley, M.H., 1983. Phosphorus in spring waters of the Taupo volcanic zone, North Island, New Zealand. *Chem. Geol.* 38, 287–306. [https://doi.org/10.1016/0009-2541\(83\)90060-8](https://doi.org/10.1016/0009-2541(83)90060-8).
- Tipping, E., Benham, S., Boyle, J.F., Crow, P., Davies, J., Fischer, U., Guyatt, H., Helliwell, R., Jackson-Blake, L., Lawlor, A.J., Monteith, D.T., Rowe, E.C., Toberman, H., 2014. Atmospheric deposition of phosphorus to land and freshwater. *Environ. Sci. Process. Impacts* 16, 1608–1617. <https://doi.org/10.1039/c3em00641g>.
- Turunen, J., Roulet, N.T., Moore, T.R., Richard, P.J.H.H., 2004. Nitrogen deposition and increased carbon accumulation in ombrotrophic peatlands in eastern Canada. *Global Biogeochem. Cycles* 18, 1–12. <https://doi.org/10.1029/2003GB002154>.
- Urrutia, R., Araneda, A., Cruces, F., Torres, L., Chirinos, L., Treutler, H.C., Fagel, N., Bertrand, S., Alvia, I., Barra, R., others, 2007. Changes in diatom, pollen, and chironomid assemblages in response to a recent volcanic event in Lake Galletué (Chilean Andes). *Limnol. Manag. Int. Waters* 37, 49–62.
- Walbridge, M.R., Navaratnam, J.A., 2006. Phosphorus in boreal peatlands. In: Wieder, R.K., Vitt, D.H. (Eds.), *Boreal Peatland Ecosystems*. Springer Berlin Heidelberg, pp. 231–258. [https://doi.org/10.1007/978-3-540-31913-9\\_11](https://doi.org/10.1007/978-3-540-31913-9_11).
- Wang, M., Moore, T.R., Talbot, J., Richard, P.J.H., 2014. The cascade of C:N:P stoichiometry in an ombrotrophic peatland: from plants to peat. *Environ. Res. Lett.* 9 <https://doi.org/10.1088/1748-9326/9/2/024003>.
- Wang, M., Moore, T.R., Talbot, J., Riley, J.L., 2015a. The stoichiometry of carbon and nutrients in peat formation. *Global Biogeochem. Cycles* 29, 113–121. <https://doi.org/10.1002/2014GB005000>. Received.
- Wang, R., Balkanski, Y., Boucher, O., Ciais, P., Peñuelas, J., Tao, S., 2015b. Significant contribution of combustion-related emissions to the atmospheric phosphorus budget. *Nat. Geosci.* 8, 48–54. <https://doi.org/10.1038/ngeo2324>.
- Wilson, C.J.N., Gravelly, D.M., Leonard, G.S., Rowland, J.V., 2009. Volcanism in the central Taupo Volcanic Zone, New Zealand: tempo, styles and controls. *Stud. Volcanol. Leg. Geogr. Walker. Spec. Publ. IAVCEI* 2, 225–247.
- Wolejko, L., Ito, K., 1986. Mires of Japan in relation to mire zones, volcanic activity and water chemistry. *Jpn. J. Ecol. (Tokyo)* 35, 575–586.
- Wolff-Boenisch, D., Gislason, S.R., Oelkers, E.H., Putnis, C.V., 2004. The dissolution rates of natural glasses as a function of their composition at pH 4 and 10.6, and temperatures from 25 to 74 °C. *Geochem. Cosmochim. Acta* 68, 4843–4858.
- Worrall, F., Moody, C.S., Clay, G.D., Burt, T.P., Rose, R., 2016. The total phosphorus budget of a peat-covered catchment. *J. Geophys. Res.: Biogeosciences* 121, 1814–1828. <https://doi.org/10.1002/2016JG003375>.
- Yafa, C., Farmer, J.G., 2006. A comparative study of acid-extractable and total digestion methods for the determination of inorganic elements in peat material by inductively coupled plasma-optical emission spectrometry. *Anal. Chim. Acta* 557, 296–303. <https://doi.org/10.1016/j.aca.2005.10.043>.
- Yu, Z., 2011. Holocene carbon flux histories of the world's peatlands: global carbon-cycle implications. *Holocene* 21, 761–774. <https://doi.org/10.1177/0959683610386982>.
- Yu, Z.C., 2012. Northern Peatland Carbon Stocks and Dynamics: A Review. *Biogeosciences*. <https://doi.org/10.5194/bg-9-4071-2012>.
- Zawalna-Geer, A., Lindsay, J.M., Davies, S., Augustinus, P., Davies, Sarah, 2016. Extracting a primary Holocene cryptotephra record from Dupuke maar sediments, Auckland, New Zealand. *J. Quat. Sci.* 31, 442–457.